Catalytic Application of Metal Organic Framework towards Methanol Oxidation in Direct Methanol Fuel Cell

By

Muhammad Ammad

School of Chemical and Materials Engineering

National University of Science and Technology

2019

Catalytic Application of Metal Organic Framework towards Methanol Oxidation in Direct Methanol Fuel Cell

Name: Muhammad Ammad

Reg. No: 00000172838

This thesis is submitted as a partial fulfillment of the requirements for the degree of

MS in Chemical Engineering

Supervisor Name: Dr. Tayyaba Noor

School of Chemical and Materials Engineering (SCME)

National University of Science and Technology (NUST)

H-12, Islamabad, Pakistan

2019

Dedication

Dedicated to Almighty Allah, my beloved family, and my supervisor. It could not have been possible without them.

Acknowledgments

There is no one except Almighty Allah, whose will is necessary for everything and anything in this world, who favored us with the capacity to think and made us anxious to investigate this entire universe. Incalculable greetings upon the Holy Prophet Hazrat Muhammad (PBUH), the reason for the creation of the universe and wellspring of information and blessing for whole humankind.

I pay my sincere gratitude to Dean and Principle of SCME, Dr. Arshad Hussain for being a source of great inspiration and for facilitation of this research work. I am indebted to HOD Chemical Engineering Dr. Muhammad Bilal Khan Niazi for facilitating me throughout my course at NUST.

From the core of my heart, I am thankful to my research supervisor, Dr. Tayyaba Noor for her unwavering technical and moral support and enlightening me with a research vision and pushing me for excellence. Her quest for perfection and excellence had been a source of inspiration and driving force. It is her consistent and encouragement that empowered me to achieve the onerous milestone.

I extend my sincere gratitude towards my guidance and committee members: Dr. Sarah Farrukh and Dr. Abdul Qadeer Malik for guiding and supporting me in my research course. It would not have been possible without them. I express my gratitude for Dr. Muhammad Shahid for letting me work in Corrosion Lab and Dr. Sofia Javed for allowing me to carry out research in Nano Synthesis Lab. My thanks also goes to Mr. Muhammad Zeeshan, Mr. Malik Nouman Shahzad and late Mr. Shams-ud-din for their significant contribution.

I am highly obligated to my family for their never ending love. Thanks for believing in me, wanting the best for me and inspiring me to follow my passion. To my friend, Atif, Dooa, Muzammil and Arman thank you for your support, advice and encouragement.

Abstract

In this work, the catalytic activity of Cu-BTC which is also known as HKUST-1 has been measured towards Methanol oxidation reaction for Direct Methanol Fuel Cells (DMFC). The catalytic characteristics were enhanced when Graphene Oxide was added to Metal Organic Framework. CU-BTC was prepared via a facile hydrothermal method and Graphene Oxide was synthesized through Improved Hummer's method. (1-5)wt% of GO composites with Cu-BTC were synthesized and the concentration of GO was optimized through 8wt% GO sample. As the concentration of GO was increased, catalytic testing showed superior performance due to enhanced surface area and conductivity provided by Graphene Oxide. The Cu-BTC/8wt% GO sample displayed lower catalytic activity because higher concentration of GO blocked the pores of MOF and hindered the active catalytic sites necessary for the methanol oxidation reaction to proceed. Samples were characterized through X-ray diffraction, scanning electron microscopy, and Fourier transform infrared spectroscopy. XRD showed the crystallinity of the material and reflected that the incorporation of GO did not affect the structure of the MOF. SEM revealed the morphology and symmetry of the cubic structure of the material while FTIR hinted at the functional groups that must be present and confirms the successful synthesis. Electrochemical studies were carried out through cyclic voltammetry, Electrochemical Impedance Spectroscopy and Chronoamperometry. The sample with highest concentration of GO(Cu-BTC/ 5wt% GO) displayed highest current density of 120.23mA/cm^2 at a scan rate of 50mV/s, it also had the lowest charge transfer resistance(R_{ct}) and highest capacity of 54% for retaining current over prolonged period of time as illustrated by chronoamperometry. The enhanced activity was a response of high conductive properties of GO.

Keywords: Graphene Oxide, Metal Organic Frameworks, Cu-BTC, Methanol oxidation reaction, Direct methanol fuel cells, Electrocatalysis, Hydrothermal method, Improved Hummer's method.

Table of Contents

List of figures……..…….vii

List of acronyms……..…….ix

Chapter 1: Introduction 1

1.1 Energy Crisis:..... 1

1.2 Fuel Cells: 2

1.2.1 Types Of Fuel Cells: 3

1.3 Experimental Techniques..... 12

1.3.1 Cyclic Voltammetry:..... 12

1.3.2 Electrochemical Impedence Spectroscopy: 13

1.3.3 Chronoamperometry: 15

1.3.4 Scanning Electron Microscope: 15

1.3.5 X-Ray Diffraction (XRD):..... 17

1.3.6 Fourier Transform Infrared Spectroscopy: 17

1.4 Synthesis Methods: 18

1.4.1 Hrdrothermal Method: 18

1.4.2 Hummers Method: 19

1.5 Current Impediments For DMFC: 20

1.6 Problem Statement:..... 21

1.7 Research Objectives:..... 22

Chapter 2: Literature Survey 23

2.1 Requirement Of Substitue Catalyst:..... 23

2.2 Electrocatalyst For Dmfc:..... 23

2.2.1 Platinum Based Catalyst: 23

2.2.2 Platinum Based Alloy: 23

2.2.3 Platinum/Metal Oxide Based Catalyst: 24
2.2.4 Nanotubes Based Electrocatalyst For MOR: 24
2.2.5 Nanoparticles Of Platinum-Metal Alloy Based Electrocatalysts For MOR: ... 25
2.3 Metal Organic Framework For Energy Applications: 26
2.3.1 Gas Storage: 26
2.3.2 Carbon Dioxide Capturing: 27
2.3.3 Proton Conductivity For Fuel Cell Applications: 27
2.3.4 Mof Nanocrystals: 27
2.3.5 Catalytic Activity Of MOF: 28
2.4 Areas Unexplored: 28
Chapter 3 Experimentation 29
3.1 Synthesis Of Catalysts 29
3.1.1 Synthesis Of Cu-BTC: 29
3.1.2 Synthesis Of Graphene Oxide: 29
3.1.3 Synthesis Of Cu-Mof/Go Composites: 30
3.2 Electrochemical Set Up 30
3.2.1 Preparation Of Working Electrode (GCE) 30
Chapter 4 Results And Discussions 31
4.1 Sample Characterization 31
4.1.1 X-Ray Diffraction Pattern 31
4.1.2 Scanning Electron Microscopy 32
4.1.3 Fourier Transform Infrared Spectroscopy: 39
4.2 Electrochemical Characterization: 40
4.2.1 Cyclic Voltammetry: 40
4.2.2 Study Of Effect Of Scan Rate: 42

4.3 Electrochemical Impedence Spectroscopy: 48

4.4 Chronoamperometry: 51

Conclusion……...……..52

Future Recommendations……...53

References……...……..54

List of Figures

Figure 1: Schematic diagram of PEMFC……. ……4
Figure 2: Schematic diagram of AFC……5
Figure 3: Schematic diagram of PAFC……..……7
Figure 4: Working principle of MFC…….……8
Figure 5: Working principle of SOFC……9
Figure 6: Schematic diagram of DMFC…….……..……11
Figure 7: A conventional voltammogram……..……..…12
Figure 8: EIS curves……..……...…14
Figure 9: Chronoamperometric curves……..……..15
Figure 10: Working of SEM……16
Figure11: Working diagram of FTIR……. 18
Figure 12: XRD patterns of Cu-BTC and composites with GO……..…31
Figure 13: SEM images of GO……32
Figure 14: SEM images of Cu-BTC……33
Figure 15: SEM images of Cu-BTC/1wt% GO……...……33
Figure 16: SEM images of Cu-BTC/2wt% GO ……..……34
Figure 17: SEM images of Cu-BTC/3wt% GO ……..……35
Figure 18: SEM images of Cu-BTC/4wt% GO ……..……36
Figure 19: SEM images of Cu-BTC/5wt% GO ……..……37
Figure 20: SEM images of Cu-BTC/8wt% GO ……..……38
Figure 21: FTIR spectra of Cu-BTC and composites with GO……39
Figure 22: CV of bare electrode……...……40
Figure 23: Comparison of CV results among different samples……..……41

Figure 24: Effect of scan rate on current density of Cu-BTC…… ……43

Figure 25: Effect of scan rate on current density of Cu-BTC/1wt% GO……43

Figure 26: Effect of scan rate on current density of Cu-BTC/2wt% GO ...……44

Figure 27: Effect of scan rate on current density of Cu-BTC/3wt% GO ...……45

Figure 28: Effect of scan rate on current density of Cu-BTC/4wt% GO ……...……46

Figure 29: Effect of scan rate on current density of Cu-BTC/5wt% GO ……47

Figure 30: Effect of scan rate on current density of Cu-BTC/8wt% GO ……49

Figure 31: EIS curves of Cu-BTC and composites with GO……...……50

Figure 32: Nyquist plot for various concentration of catalyst…….……51

Acronyms

MOF: Metal Organic Framework

GO: Graphene Oxide

CV: Cyclic Voltammetry

Pt: Platinum

XRD: X-Ray Diffraction

SEM: Scanning Electron Microscopy

kW: Kilo Watt

MOR: Methanol Oxidation Reaction

MFC: Microbial Fuel Cell

HER: Hydrogen Evolution Reaction

CD: Current Density

DMFC: Direct Methanol Fuel Cell

DMF: Dimethyl Formamide

MCFC: Molten Carbonate Fuel Cell

RDE: Rotating Disk Electrode

GCE: Glassy Carbon Electrode

SCE: Standard Calomel Electrode

AC: Alternating Current

RE: Reference Electrode

TEA: Triethyl Amine

kV: Kilo Volt

FTIR: Fourier Transform Infrared Spectroscopy

ORR: Oxygen Reduction Reaction

CNT: Carbon Nanotube

OER: Oxygen Evolution Reaction

BTC: Benzene Tricarboxylate

SOFC: Solid Oxide Fuel Cell

POFC: Phosphorus Oxide Fuel Cell

rGO: Reduced Graphene Oxide

CE: Counter Electrode

CHAPTER 1

Introduction

1.1 Energy Crisis:

The requirement of energy is a direct indication of well-being and prosperity of a country. It drives the country and is a source of fulfilling basic needs of human being. Be it as basic as cooking food, lightening a room or pumping water from underground to highly sophisticated and complex industrial processes, we need energy of all forms in every walk of life. It has been estimated that a rise of 10% in energy consumption is proportional to 1.56% hike in economic growth.[1]

The sources of energy can be broadly categorized into two: non-renewable and renewable sources. Non-renewable sources are the ones which cannot be reformed or reproduced in a limited timeframe. The major sources are crude oil, natural gas, coal, and Uranium.[2]

On the other hand, the sources of energy which are not depleted with time and remain useable are called renewable source of energy. The common types are biomass, hydrothermal, geothermal, wind, solar, and electrochemical forms.

Since the industrial revolution, there has been an immense hike in energy demand due to continuous expansion of industrial production. The exponential proliferation of world's population and rising living standards of human beings have added more pressure on the limited recourses of fuel.

According to a survey in 2013[3], 82.5% of world's energy is produced from fossil fuel, amongst which 86.59% is generated from oil, 30% is extracted from coal, and 23.72% is taken from coal. This ever increasing demand has overburdened the current fossil fuel reserves and geologists are fearing that if the reserves are being consumed with the same pace, the menace of huge energy crisis is inevitable, given that a feasible alternate to conventional source of energy is not being sought. On indigenous level, in 2013, the total energy supply to Pakistan was 64.5 million tons of oil equivalent (MTOE). The fraction contributed by gas was 48.2%, oil's share was 32.5%, coal 6%, and Liquid Pressurized gas (LPG) used was 0.5% of the total consumption[4]. As Pakistan's indigenous reservoirs cannot meet its demands, it has to import crude oil worth billions of dollar

which is aggravating the already wounded economic condition of Pakistan. Apart from the financial point of view, the use of fossil fuels is highly hazardous to environment. The combustion of oil produces Carbon Monoxide, Sulfur oxides, and Nitrogen Oxides which are highly poisonous and pose major threat as a pollutant to air, water and land. To deal with the issue of depleting reserves of fossil fuels and address the prevailing pollution require the development of inexpensive and environmental friendly means of energy which is easily available to everyone. The conventional sources of fuel, fossil fuel, are depleting at a rapid pace due to massive requirement of energy for industrial purposes. This huge demand of supply is creating a supply-demand gap which is widening day by day. To address this issue, we need to go towards alternate source of energy which keeps the balance between the two and must be environment friendly. Keeping these points in mind, fuel cell is considered to be highly efficient, clean and promising energy resource with higher current densities as compared to other alternatives.

1.2 Fuel Cells:

An electrochemical device that transforms chemical energy of ongoing redox reaction into electrical energy is called fuel cell. It is popular for its environmentally benign characteristics and releases only water (H_2O) as a by-product, except in the case of Direct Methanol Fuel Cells (DMFC) where Carbon Dioxide (CO_2) and water are obtained as end products along with desired energy. Fuel cells largely resemble to the common portable batteries in mechanism but the fuel supply of the batteries, i.e the chemicals required to carry out the redox reaction are deposited only once at the time of manufacturing and when the battery runs out of chemicals, it becomes obsolete. Therefore, batteries are disposable. On the other hand, fuel cell is just an electrochemical reaction chamber that requires periodic supply of fuel Oxygen and Hydrogen to produce electricity. A rudimentary form of fuel cells consists of following components:

- A cathode where Oxygen gets reduced to form water.
- An anode where oxidation of Hydrogen occurs.
- An electrolyte that facilitates the flow of ions. It varies with the type of cell used and operating conditions such as temperature, power output, and end application.

Although fuel cells seem to be very attractive and fascinating technological advancement, there are still many hurdles in the way of its day-to-day life. Though Oxygen can be extracted from air, there are still no sources for readily available Hydrogen and it is obtained through reforming of

natural gas which itself is a process harmful to climate. Another problem that halts the commercialization of fuel cells is the development of an efficient and inexpensive catalyst to speed up the reaction at both electrodes. Till now, that only material that has performed upto the mark as a catalyst is Platinum. It delivers reliable performance but its exorbitant price and lack of abundance make it a weak candidate as a catalyst.

The concept of fuel cells dates back to early nineteenth century when the initial studies of electricity and its origin were being conducted. A British scientist Sir Humphry Davy experimented that when electricity is passed through water, it splits into Oxygen and Hydrogen. This process is now called electrolysis. Later that year, a German Scientist Christian Friedrich Schonbein and an English Scientist William Groove independently hypothesized that if electric current could split water into its elemental form, then the reverse reaction could produce electricity, i.e when Oxygen molecule is made to react with Hydrogen, it yields water and energy[5].

1.2.1 Types of Fuel Cells:

Fuel cells are divided into following groups based on the electrolyte they use and operating parameters[6]:

- Proton exchange membrane fuel cell (PEMFC)
- Alkaline fuel cell (AFC)
- Phosphoric acid fuel cell (PAFC)
- Microbial fuel cells (MFCs)
- Solid Oxide fuel cells (SOFCs)
- Direct Methanol fuel cell (DMFC)

1.2.1.1 Proton Exchange Membrane Fuel Cell (PEMFC):

It uses polymeric membranes based on water as an electrolyte for the smooth transfer of protons and electrode material is usually Platinum. Pure Hydrogen gets oxidized at the positive electrode which is attached electrically to the outer circuit. Hydrogen losses the electrons at the anode which passes through the outer circuit, while the positive ions move though the polymer membrane to reach the cathode. Oxygen at the negative electrode reacts with Hydronium ions and electrons to form water.

At anode: $H2 \rightarrow 2(aq) + 2e^-$

At cathode: $1/2O_2 + 2_{(aq)+} + 2e^- \longrightarrow H_2O$

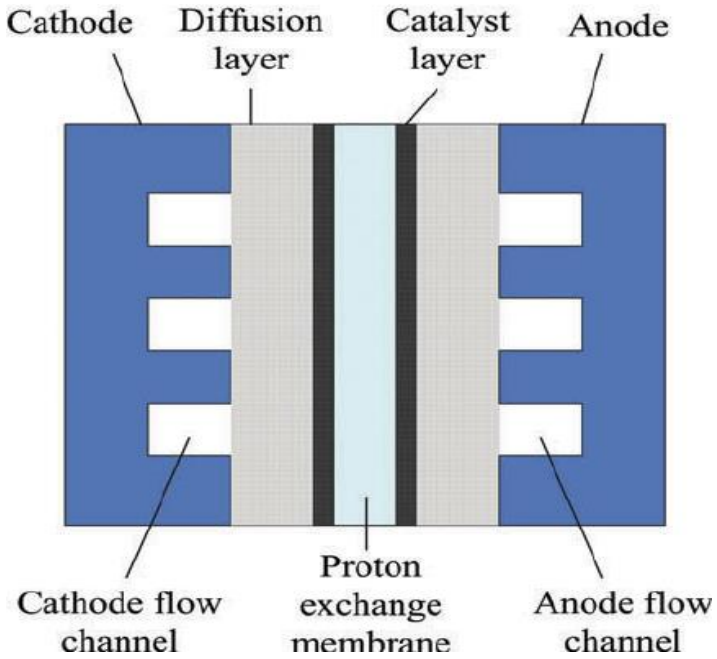

Figure 1: Schematic of PEMFC

PEMFC finds its applications in both light vehicles as well as transportation vehicles. They are also referred to as polymer electrolyte membrane fuel cells. They are available in two variants according to the operating temperature [8] :

- Low temperature PEMFC which employs water based polymeric membranes and operates at a temperature below 100 degree celcius.
- High temperature PEMFC that ultilizes mineral based polymeric membrane as an electrolyte and is functional at up to 200 degree celcius.

1.2.1.2 Alkaline Fuel Cells:

This type of fuel cell employs Potassium Hydroxide (KOH) or Sodium Hydroxide (NaOH) as an electrolyte and uses cheap electrode material. They are effective in a wide range of temperature and can operate in 50-200 degree Centigrade. They were first of the kind that were used by NASA in Apollo and other space shuttle mission.

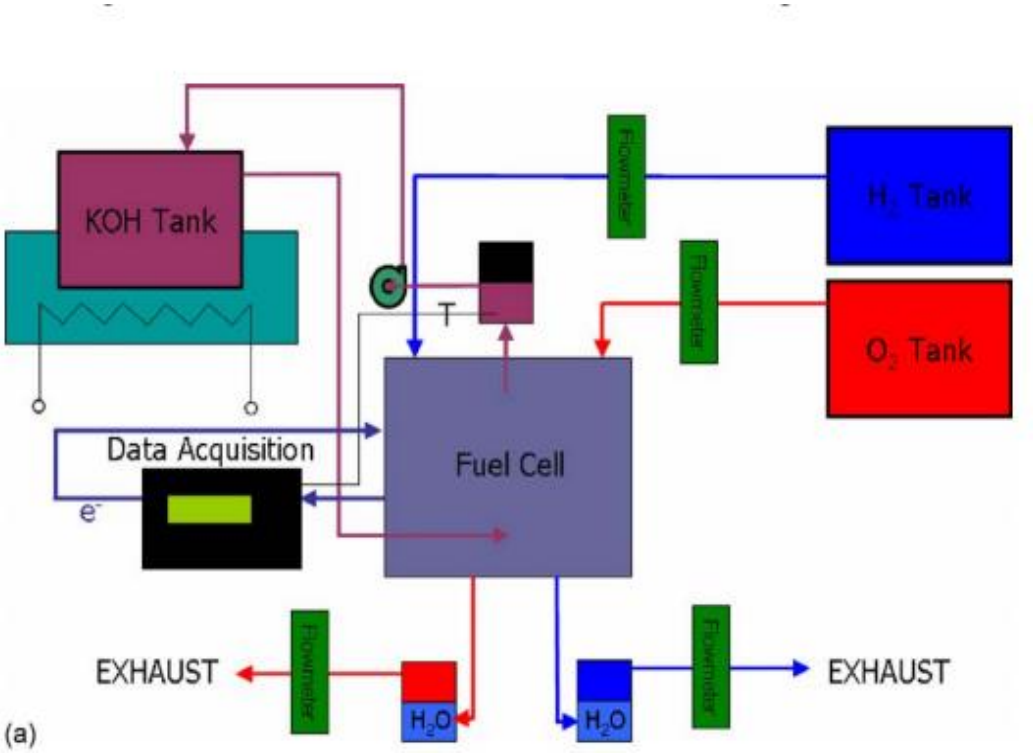

Figure 2: Schematic of Alkaline fuel cell [9]

The mechanism of AFC is quite simple. Hydrogen at the anode losses electron to get oxidized. The electrons travel through external source to reach cathode while Hydrogen ions are sucked into the electrolyte where they react with Hydroxyl ions to form water. The Oxygen, extracted from air, receives electrons at the anode to be reduced to Hydroxyl ions and jumps into pool of electrolyte to combine with Hydronium ions to produce water.

At anode: $2H2(g)+4OH-\longrightarrow 4\ H2O(l)+4e-$

At cathode: $O2(g)+2H2O(l)+4e-\longrightarrow 4OH-$

Although, AFC have appreciable efficiency and reliability, they have few shortcomings that bar them from successful operation. Firstly, they are easily poisoned by Carbon dioxide and

secondly, there hasn't been developed a reliable barrier that prevents the leakage of reactants from the electrode.

1.2.1.3 Phosphoric Acid Fuel Cell:

It is composed of two porous gas diffusion electrodes: air electrode (cathode) and fuel electrode (anode) both made of carbon material. Between the electrodes, entrapped is an electrolyte which consists of matrix containing highly concentrated Phosphoric acid. It is extremely stable and can be easily handled. At the anode, Hydrogen reacts at the catalyst surface to give Hydrogen ions and electrons, the protons migrate through the electrolyte to arrive on cathode. The Oxygen reacts with Hydrogen ions from anode and electrons from external circuit to form water.

Fuel Electrode: $H_2 \rightarrow 2H^+ + 2e$

Air electrode: $(1/2)O_2 + 2H^+ + 2e^- \rightarrow H_2O$

A single cell produces a voltage between 0.6- 0.8V. Therefore, for practical applications, hundreds of cells are piled together to obtain the required voltage for the desired purpose. PAFC is not harmed by catalyst poisoning as observed in alkaline fuel cells. Therefore, Hydrogen can be easily extracted by reforming of natural gas.

PAFC employs Phosphoric acid as an electrolyte and the electrode most commonly used is Platinum based. Although, Platinum does not get poisoned in this setup but the insufficient ionic conductivity of the acid renders the electrode poisonous and make it suspicious towards decrease in efficiency. PAFC functions at a relatively high temperature of 420K to 500K and therefore not exactly suitable for day-to-day application. Although, it has been used for commercial vehicles such as buses but there are quite a few companies who are still using this technology and manufacturing the devices.

In 1970 first phosphoric acid fuel cell power plant was installed and now there are about 500 such working power plants in the world. They are considered good for stationary applications.

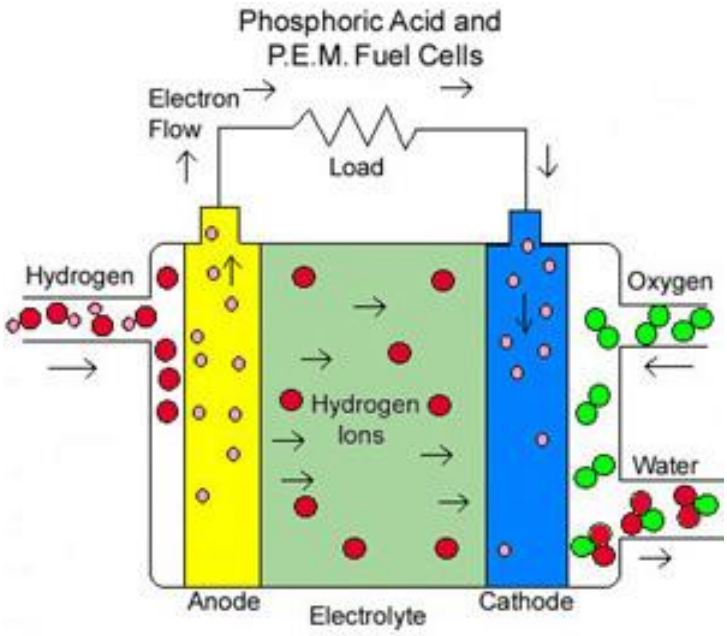

Figure 3: Schematic of Phosphoric acid fuel cell (PAFC) [10]

1.2.1.4 Microbial Fuel Cells:

The type of fuel cell that uses organic substrate as a fuel and active microorganisms as biocatalyst is called microbial fuel cell. It is largely similar in mechanism to ordinary fuel cell but it adopts biological sources for provision of energy instead of conventional chemically catalyzed reaction.

A typical MFC contains an anode and cathode. The electrodes are isolated by proton exchange membrane (PEM) which acts as an electrolyte. Protons and electrons are produced at the anode by the anaerobic oxidation of organic substrate with the help of bacteria. The condition of non-availability of Oxygen here is mandatory because it prevents the bacteria to oxidize or reduce organic substances. The protons are transferred to the cathode through PEM while electrons are transported to the cathode by external circuit. The Oxygen at the cathode reacts with Hydronium ions and electrons to give off water, the sole byproduct of the reaction. Based on the collection of electrons from the organic material to the electrode, MFCs can be classified into mediator and mediatorless microbial fuel cells.[11]

The reactions occurring at the electrodes are:

ANODE: $CH_4O_2 + 2H_2O \rightarrow 2CO_2 + 8e^- + 8H^+$

CATHODE: $2O_2 + 8H^+ + 8e^- \rightarrow 4H_2O$

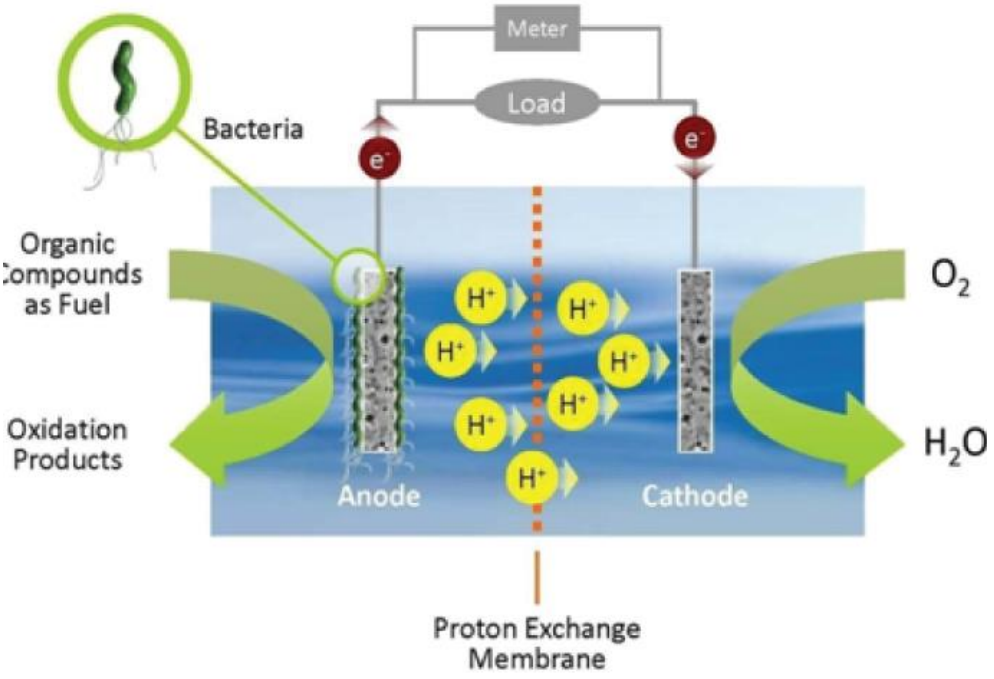

Figure 4: Schematic representation of Microbial fuel cell.[12]

1.2.1.5 Solid Oxide Fuel Cell:

SOFCs provide clean and green, low pollutant, and environmentally sustainable form of renewable energy. It supports the cause of protecting the climate by emitting minimal amount of NOx, SOx, and oxides of Carbon. It has the potential to indigeniously carry out the reforming of fuel such as Natural gas for the supply of Hydrogen. The operating temperature of SOFCs is usually 700-1000C [13]. The maximum efficiency that has been achieved so far is around 70% and the exhaust gases can f be utilized to run the turbine at the power stations which can further elevate the overall efficiency.

SOFCs normally consist of two porous electrodes separated by dense, oxide ion conducting electrolyte. Oxygen at the cathode reacts with the electrons from external circuit to produce oxide ions. These ions travel through the electrolyte to combine with Hydrogen to release water along

with the liberation of electrons. Tradition materials that are used as oxide ion conduction electrolyte are Yttria-doped Zirconia (YSZ) and Scandia doped Zirconia. [14]

At cathode: $O_2 + 4e \rightarrow 2O^{--}$

At anode: $2H_2 + 2O^{-} \rightarrow 4e^{-} + 2H_2O$

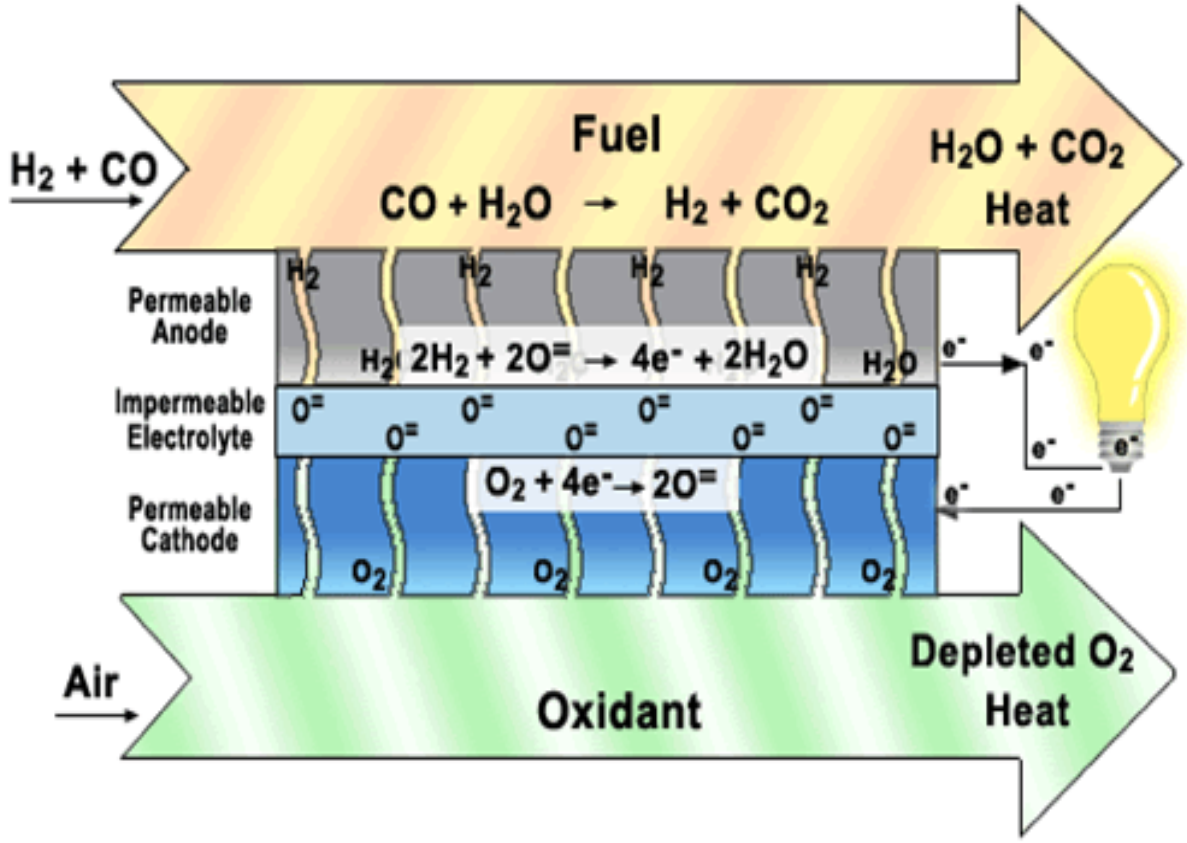

Figure 5: Working principal of Solid Oxide fuel cell. [14]

1.2.1.6 Direct Methanol Fuel Cells:

The type of fuel cells that uses methanol as fuel to transform the chemical energy into electrical energy through an electrochemical reaction is called Direct Methanol Fuel Cell. It differs from the

rest of fuel cell family in regards to the fuel usage. While rest of the fuel cell setups either require Natural gas or rely some other source for their Hydrogen needs fulfillment, DMFC only needs methanol as its sole requirement for its efficient functioning. The fact that all other types of fuel cells require fossil fuel for the provision of Hydrogen undermine their real purpose of generating clean and environmentally benign energy because the products of combustion of fossil are the primary pollutants. The facile transportation and easy handling coupled with the high energy density (6.1kWh/kg) of methanol makes it much superior in performance than the conventional Lithium ion battery.

DMFCs can be classified into three catagories according to the manner in which methanol and Oxygen is supplied:

Active DMFC in which methanol and oxidant are supplied through motors, fans, and pumps etc.

- Passive DMFC that does not use any additional instruments for supply of methanol and Oxygen and are carried to the Methanol electrode assembly (MEA) though gravity, capillary forces, and concentration gradient.
- Semi passive DMFC is a hybrid of the two above, it may employ passive mode at anode and active style at cathode or vice versa.

The mechanism of DMFC is relatively simple. It consists of two metal electrodes isolated by an basic electrolyte, typically Sodium Hydroxide (NaOH) or Potassium Hydroxide (KOH). Methanol and water is provided at the anode end where methanol is electro-oxidized to CO_2 and Hydronium ion and electrons are liberated. Hydrogen ions move through the electrolyte to the negative electrode while electrons arrive at the same destination via outer circuit connecting both the electrodes. Oxygen at the cathode meet with Hydrogen ions and electrons to generate water.

The reaction occuring at the electrodes are given below:

ANODE: $CH_3OH + H_2O \rightarrow CO_2 + 6H^+ + 6e^-$

CATHODE: $3/2O_2 + 6H^+ + 6e^- \rightarrow 3H_2O$

Net Reaction: $CH_3OH + 3/2O_2 \rightarrow CO_2 + 2H_2O$

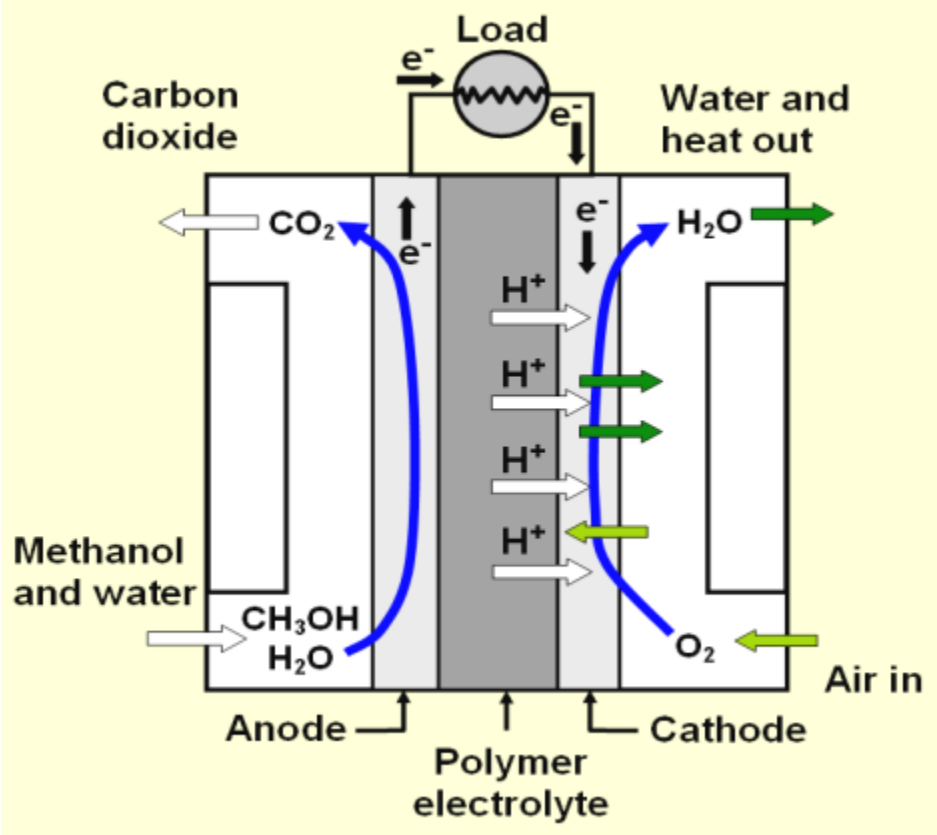

Figure 6: Working principal of Direct Methanol Fuel Cell [15].

DMFCs have huge prospects in portable elecronic devices such as communication devices, laptops etc as well as it possess bright future in light electric vehicles.

Currently, two majors hurdles are barring the commercializing of DMFCs. First being the issue ofMethanol crossover and the second one is high cost due to expensive catalyst used for methaol oxidation and Oxygen evolution reactions. Commercial units of fuel cells use Platinum as a catalyst, which is really expensive and cost-inefficient. Research is being extensively conducted at non-noble metals as an alternate catalyst, which include Nickel, Copper, Ruthernium etc.

Among Carbon materials, Grahpene and Graphene oxide are serious compitetors. An emerging material in the field of nano-sciences is Metal Organic Framework (MOF) which has shown a great potential as an electrocatalyst due to its surface area, consistent performance in wide range of temperature, and high structural integrity.

1.3 Experimental Techniques

1.3.1 Cyclic Voltammetry:

Cyclic voltammetry is the most efficient technique to obtain qualitative information about electrochemical reactions. It can also be used to measure kinetic path of electrode reactions, where electrode reaction usually involves electron-transfer reaction which is influenced by electrode potential. Principally, in this technique, a fixed potential electrode is used to provide a given voltage to the working electrode to push the reaction forward while the axillary electrode completes the circuit by collecting the electrons.

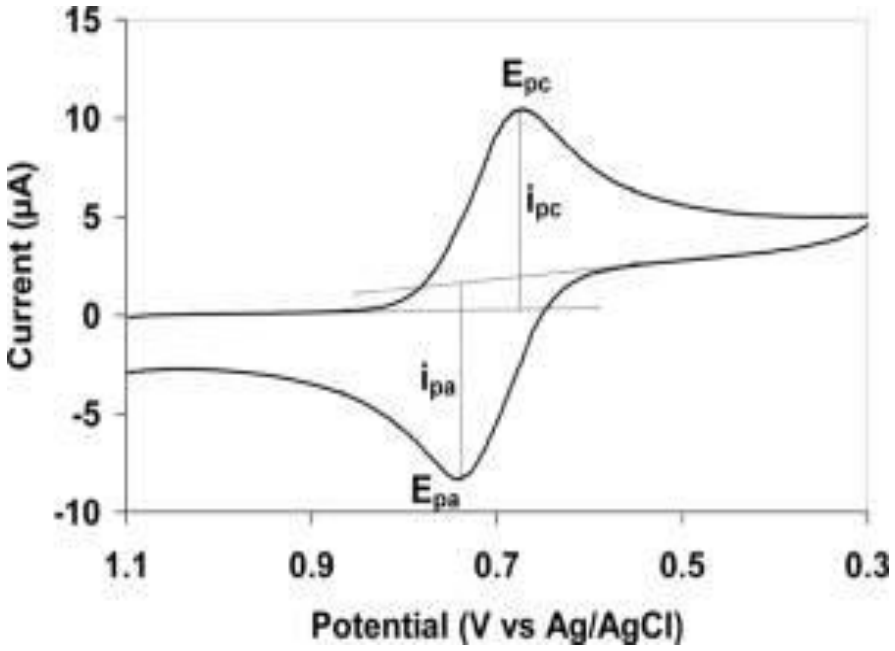

Figure 7 :A conventional voltammogram.

The main purpose of cyclic voltammetry is to study the electrochemical properties of an analyte in solution. In a cyclic voltammetry experiment, there is an electrochemical cell containing three electrodes namely reference electrode, counter electrode and working electrode.In an electrochemical cell, these three electrodes are put together in an electrolyte solution that usually contain an electroactive species.

Working electrode is the electrode in cyclic voltammetry experiment, where reaction of our interest occurs. Gold, silver, platinum, and glassy carbon are usually considered as working electrode materials. There are some other special types of working electrodes such as rotating ring-disk electrode, rotating disk electrode, dropping mercury electrode and ultra-microelectrode. Reference electrode is the electrode which has a stable electrode potential. There are various types of reference electrodes such as saturated calomel electrode, copper-copper (II) sulfate electrode, silver chloride electrode and silver-silver chloride electrode. Counter electrode is the electrode in an electrochemical system where flow of electric current is expected. Platinum, gold and carbon are the commonly used materials for counter electrode.

In cyclic voltammetry potential is usually applied between the reference electrode and working electrode, whereas current is observed between the counter and working electrode.

Electrolyte is usually added to provide sufficient conductivity. In cyclic voltammetry solvent, electrolyte and working material determines the range of potential that can be observed during experiment.

Cyclic voltammetry has been widely used as an electroanalytical technique in various fields of chemistry. Cyclic voltammetry is used to determine electron transfer kinetics, various redox processes, reversibility of the reaction and electron stoichiometry of a system. It can also be used to determine diffusion coefficient of an analyte and as an identification tool. Concentration of solution which is unknown can also be determined through cyclic voltammetry.

1.3.2 Electrochemical Impedance Spectroscopy:

The measure of capability of the circuit to resist the flow is called impedance. This refers to the frequency dependent resistance. It is given by AC current of a specific frequency in hertz.

$$z\omega = E\omega / I\omega \qquad (\omega = Frequency)$$

EIS measurements are done by applying sinusoidal voltage or current at a fixed frequency range and then the response in observed at each frequency [84]. Impedance is represented as a complex number given by;

$$(\omega) = E/I = Zo\exp(j\emptyset) = Z(cos\emptyset + jsin\emptyset)$$

EIS data are either presented as a Bode plot or Nyquist plot. Mostly impedance studies take Nyquist plot into consideration. A typical Nyquist plot is given in figure below

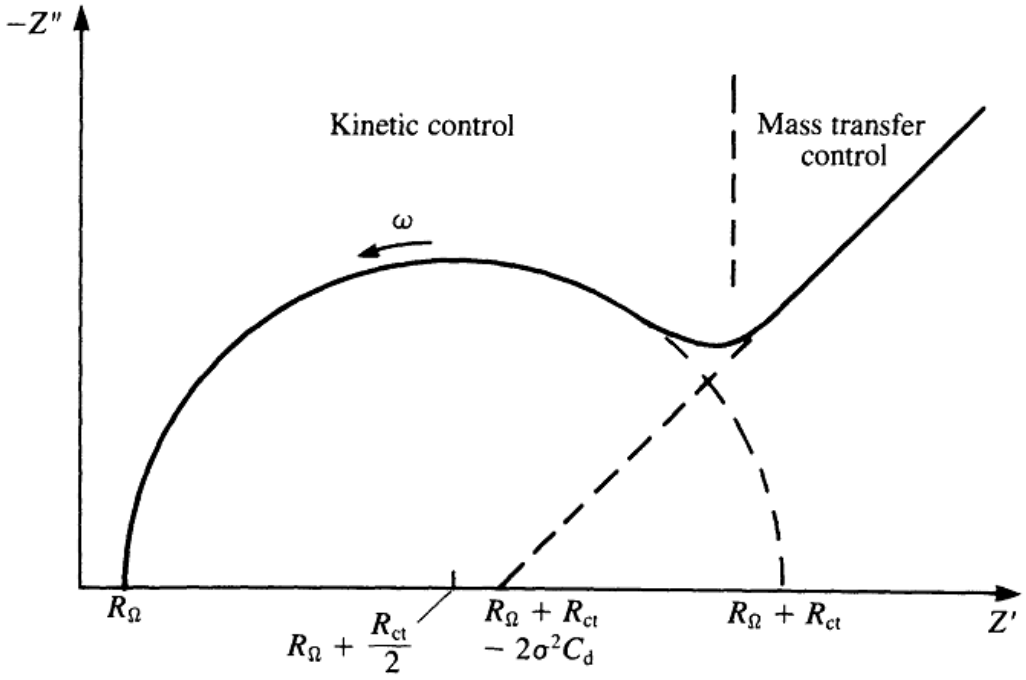

Figure 8: EIS Curves

EIS information helps to differentiate between electrochemical processes. It can help identify diffusion-limited processes. It provides information about the capacitive behavior of the electrode. Thus giving off information about the overall reaction rate of the electrochemical process occurring on that electrode. It is also useful in corrosion studies of the metallic electrodes.

1.3.3 Chronoamperometry:

This technique is used to study the stability of a catalyst in electrochemical studies. Same equipment is utilized as for CV and EIS. Prolonged period of time for chronoampermetry is required to find out the suitability and consistency of the material. It is carried out at a single fixed potential for a given time.

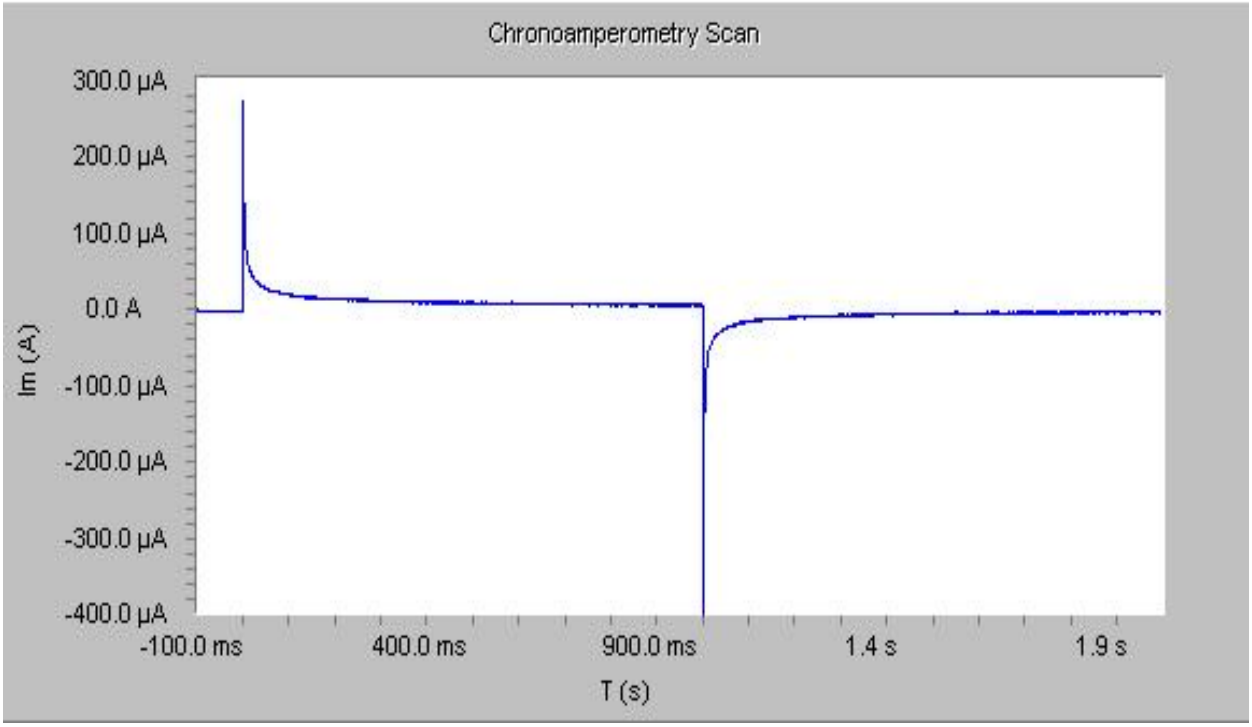

Figure 9: Chronoamperometric graph.

1.3.4 Scanning Electron Microscope:

SEM (scanning electron microscopy) is a microscope that basically uses electron instead of lhight to form an image. Scanning electron microscopy was developed in early 1950's. The main components of Scanning Electron Microscopy are scanning system, detectors, electron column, vacuum system, and display and electronics control[16]. The electron column of SEM (Figure 1.12) consists of an electron gun and two or more electromagnetic lenses. The electron gun of the electron column generates electrons and accelerates them to energies in the range from 1 to 40 keV in the Scanning Electron Microscopy. Whereas the main purpose of electron lenses is to create a small, focused electron probe on the specimen. There are two types of electron gun such as Field emission and thermionic gun. Thermionic is basically a material that exposes to high temperature

so that it emits electrons. While in field emission gun, a very strong magnetic field that draws electrons from the metallic tip (Usually Tungsten).

In field emission, there are two anodes, where 2KV voltage is applied to create electric field so that electron leaves the tip and second anode is used to accelerate these electrons towards microscope. Combination of these two anodes focuses the beam. Then beam is focused by a condenser lens (Electromagnetic lens) in order to form a probe. After focusing this beam is passed through an aperture which excludes electrons. If there are some inconsistencies in the beam that is corrected by stigmators and beam focused onto the sample. Then there are deflector coils that move the beam back over the sample and signal generated from each area is collected simultaneously to get the final image on the monitor.

The scanning electron microscopy works very fast, it can complete BSE, SEI and EDS analyses in less than five minutes. Scanning electron microscopy is user-friendly and easy to operate with the proper training. Scanning electron microscopy gives us morphological, topographical, and compositional information. It can also detect and analyze fractures, provide qualitative analyses, and identify crystalline structures.

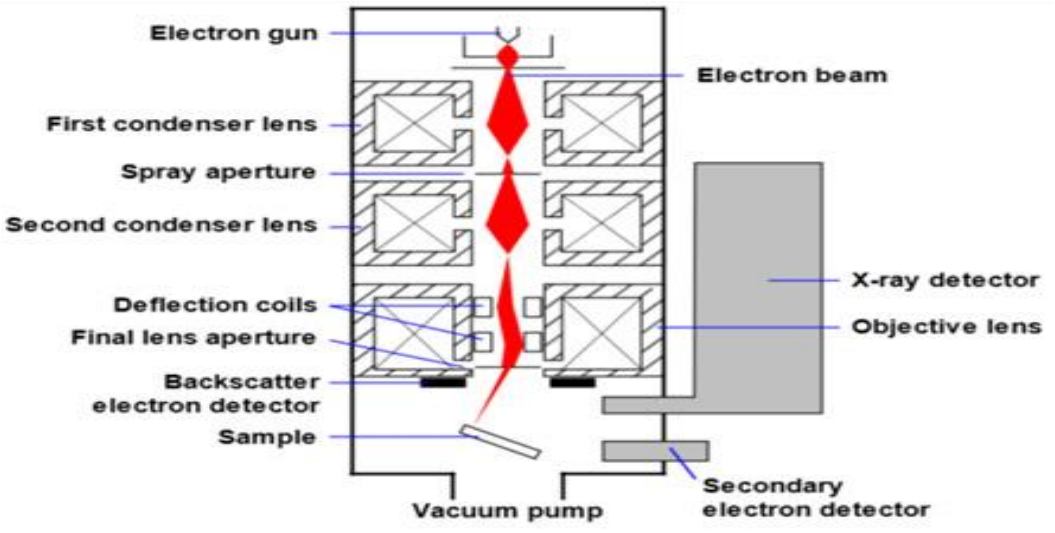

Figure 10: Working schematic of Scanning Electron Microscopy (SEM).

1.3.5 X-Ray Diffraction (XRD):

X-ray diffraction is non-damaging technique to characterize the crystallinity of the structure of the prepared electro-catalysts. Lattice parameters, size of crystallites, sample purity, unit cell dimensions and other information related to crystals can be obtained from the XRD. Basically, XRD is based on constructive interference of monochromatic X-rays and a crystalline sample[17].

These X-rays are generated by a cathode ray tube, filtered to produce monochromatic radiations (single frequency or wavelength), collimated to concentrate and directed toward the sample. The interaction of the incident rays with the sample produces constructive interference.

When condition satisfy, Bragg's law;

$$2d \sin\theta = n\lambda$$

Where; d= interlayer distance

n= number of layer under consideration

λ= wavelength

1.3.6 Fourier Transform Infrared Spectroscopy:

The infrared spectrum is another important source to study internal structure and get an idea of composition of target compounds. This technique results into a spectrum which shows bands in ranges specified for a class of compounds; functional groups [18].

This technique works best as combination with Fourier transformation. The basic principle of this technique is that the exposure of any compound to low energy infrared rays, results into change in vibration modes of dipole sites of that compound. As a result, a spectrum is formed showing the corresponding absorption or emission. These results help to evaluate the class to which that compound belongs i.e., carbonyl compound, alcoholic etc.

The basic structure and working principle of the instrument is shown as;

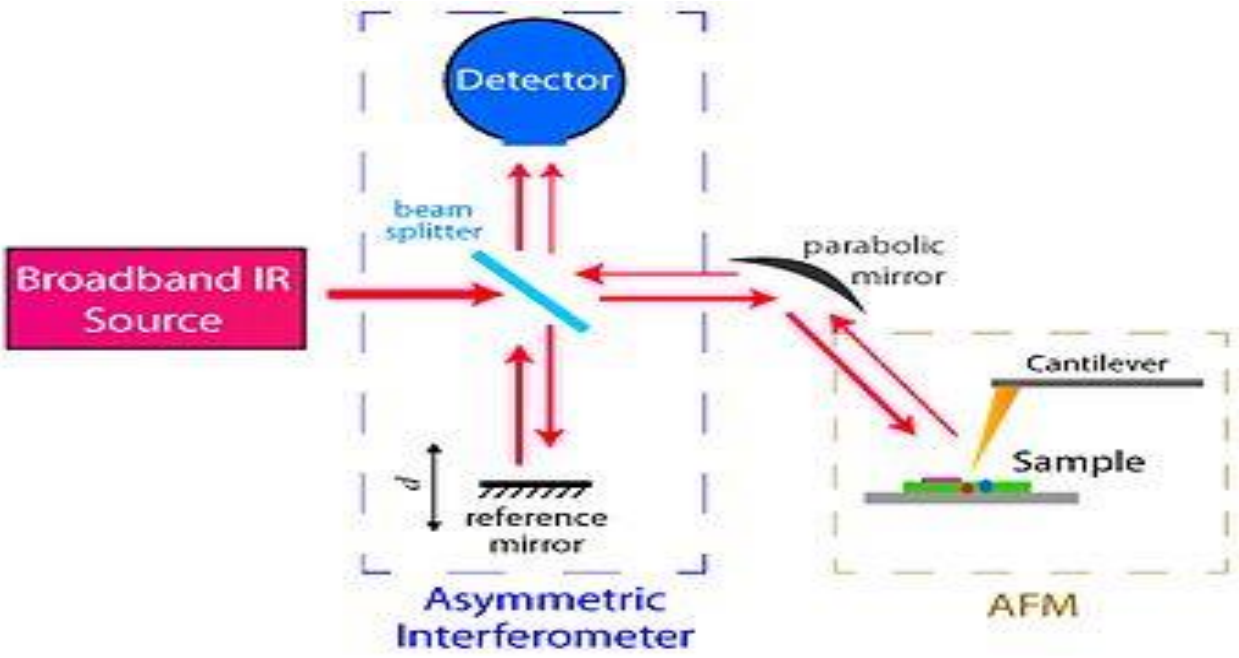

Figure 11: Working diagram of FTIR.

All these characterization techniques helped in this research to find out physical, chemical and electrochemical properties of the synthesized compounds.

1.4 Synthesis Methods:

Experimental methods adopted in this research were; hydrothermal method for making Cu-based MOF and its composites while Improved Hummers method was adopted for the manufacturing of GO.

1.4.1 Hrdrothermal Method:

The crystallization of substances at high temperature and high pressure is known as Hydrothermal Synthesis. This term finds its origin from geology. This term got to be used in the field of chemical experimentation when scientist tried to develop crystal structure at micro and macro level. Thus hydrothermal method can be defined as [19];

“Synthesis of single crystals depending upon the solubility of minerals in solvent at high temperature and high pressure”

The first growth of hydrothermally synthesized crystal was by a German geologist, Karl Emil von Schafhäutl in 1845. He performed this experiment in pressure cooker. In 1905, the growth of macroscopic crystals was reported by Giorgio Spezia [20]**.** The process follows set of rules and steps. The crystal growth is performed in the Teflon sealed autoclave which works on the same principle as that of pressure cooker. Until now, a large number of compounds have been synthesized by this method. It is helpful in synthesizing compounds of almost all classes; simple and complex compounds of oxides, carbonates, silicates etc. synthetic quartz and gems are also grown by this method. Some scientists also synthesized elemental particles via the same method.

The crystallization vessel used in this process is a strong walled vessel known as autoclave. The autoclave is made up of material which could bear high temperature, pressure and also is inert towards almost all types of compounds to avoid contamination. For the same purpose, the inside of the autoclave is protected by a layer or seal composed of inert material i.e., silver, platinum, gold, iron, copper, titanium, quartz or teflon. The autoclave after necessary filling up, is placed in a furnace known as box furnace. The crystallization is done by creating temperature difference while heating and then consequent cooling of the mixture.

1.4.2 Hummer's Method:

The chemical process of synthesizing graphitic oxide or graphene oxide by the addition of potassium permanganate, graphite, sodium nitrate and sulfuric acid into the solution is known as Hummers' method. This method is named after the scientist who first introduced this method i.e., William S. Hummers. He first developed this method in 1958 as safer, faster and more efficient method to synthesize GO [21]. This process results into the development of impure and maintaining the pH of the sample up to 7.

This process has taken up all the research in which GO is involved because it is the fastest and conventional method which maintains the ratio of carbon and oxygen in an appropriate range. Also, it produces large quantity of the product in shorter period of time. This process has taken up all the research in which GO is involved because it is the fastest and conventional method which maintains the ratio of carbon and oxygen in an appropriate range [22]. Also, it produces large quantity of the product in shorter period of time.

Small variations have been done in this method so far. One of them is the exclusion of sodium nitrate from the method. This elimination is beneficious as it stops the unnecessary formation of

nitrogen oxides. Another important variation is the introduction of exfoliation by sonication in which ultrasonic waves are used [23].

1.5 Current Impediments for DMFC:

To improve the performance of DMFCs, it is run in combination with polymer electrolyte membrane as electrolyte. Such a hybrid combines advantages of both PEMFC and DMFC. Such cells operate at low temperature and are potential candidate for almost all the applications from portable (replacing battery) to larger applications (electrical vehicles). The overall performance is also improved by implementing catalyst mainly Pt in a very less amount (down to 0.1 mg Pt/cm_2) [24].

DMFC works on the basis of membrane electrode assemblies composed proton conducting membrane such as Nafion, catalyst material, and a supporting electrolyte. Such a structure faces several obstacles:

Low activity of methanol oxidation electrocatalyst as compared to that of hydrogen

- Loss of fuel during methanol crossover from anode to cathode
- Electrode poisoning by methanol

DMFC is considered a developed form of PEMFC were PEM is the main part which provides good chemical and thermal stability. Two successful candidates in this concern are Flemion from Asahi Chemicals and Nafion from DuPont [25]. Both of them provide mechanical strength but cause high hydrophobicity of the sulfuric acid in the presence of water resulting in the methanol crossover decreasing overall performance of the system. To overcome this problem, we need to modify polymer electrolyte membrane by introducing composite materials.

Heat management is another issue to be addressed for this system because the temperature of the system increases with the increasing crossover of the fuel. This eventually reduces the overall reaction rate due to increase in the activation overpotential. This limits the rate of electrode reaction affecting the voltage efficiency of the system. This makes improving the reaction rate another obstacle to be crossed. All these aspects are currently being addressed by Chemists, Electrical Engineers, and Energy System Engineers etc. major research area covered is the improvement of

catalyst for methanol oxidation. DMFC need higher catalyst loading as compared to other fuel cell types. Pt being expensive increases the overall cost of DMFC. Thus in order to decrease this cost, we need to find an alternate which is at least close to Pt in current density profile and cheaper as well. This drives researchers to develop new anodic materials to be implied as methanol oxidation catalysts[26].

1.6 Problem Statement:

Since 2010, worldwide energy production was dominated by fossil fuels but fossil fuels are continuously depleting down to a level that experts suggests that there would be a great disaster soon if an alternative is not there to replace fossil fuels. Besides fulfilling the shortcoming of energy, we also need to find a cleaner source of energy with least emissions of harmful gases like CO_2, NO_x and SO_x. So renewable energy resources meet all these requirements. Fuel cells find the best place among all such resources. Keeping in mind the feasibilities related to fuel cell systems i.e., operating temperature, cost, reactant flow system, and mechanical setup; DMFCs is the most feasible of all the types. DMFC finds its applicability in a variety of applications such as portable electronics, microchips, power plants and in aerospace etc. The advantages of using this specific fuel cell is that it is environmentally benign and it requires less maintenance because it has no moving parts.

The main problem of DMFC is the lower power density. This is because of the poor kinetics of the electrode reaction which needs a suitable catalyst to be implemented on electrode. One best material until now is platinum which is a noble metal and very expensive eventually increasing the overall cost of the cell. The main issue associated with using Platinum as an electrode material is getting poisoned by the intermediate species which are formed during the oxidation of methanol which strongly lessen the efficacy of the catalyst. So the whole story gets to revolve around finding a catalyst which could provide good current densities and is economical as well. For this purpose, non-noble metal based catalysts are introduced for example, Cobalt (Co), Nickel (Ni), Lead (Pb), 25 Tungsten (W) etc. Similarly some research is based on Pt alloys with other metals like Ru as well in acidic media but until recent years, research is mostly bent towards introducing high surface area porous structures in catalysts. For this purpose nanomaterials and metal organic framework (MOF) have found its applications as electrocatalysts in DMFC for oxygen reduction reaction

(ORR), hydrogen evolution reaction (HER), hydrogen oxidation reaction (HOR) [27]. Nanomaterials like graphene, functionalized graphene, nanotubes, and mesoporous carbon materials act to enhance the overall surface area of the catalyst material. Metal organic framework acts as two dimensional, and three dimensional porous structures with great electrical properties. Here we combine the uniqueness of graphene oxide (GO) and metal organic framework (MOF) to be implemented as electrocatalyst for methanol oxidation in DMFC for better efficiency. The high surface area of graphene Oxide and immense porosity of Cu-BTC provides easy passage and wide channel for the electroactive species to reach central metal atom which acts as a catalyst to boost the reaction.

1.7 Research Objectives:

This research is based on following objectives;

• To synthesize graphene oxide by Hummers method

• To synthesize Copper based metal organic framework using Trimesic acid as organic linker by hydrothermal method which has been used many times for making frameworks for fuel cell

• To synthesize Cu-MOF/GO composites following the same hydrothermal method

• To characterize the synthesized material via XRD, SEM and FTIR to indicate the appropriate synthesis

• To scrutinize the electrochemical properties of synthesized catalysts via cyclic voltammetry for methanol oxidation reaction in DMFC to thoroughly compare the results of other reported materials.

CHAPTER 2

Literature Survey

2.1 Requirement of Substitute Catalyst:

One of the major challenges being faced by DMFCs regarding its improved performance is inadequate and inefficient catalyst for the reactions of oxidation of methanol occurring at anode and Oxygen reduction taking place at cathode. The decomposition products of methanol causes a great deal of damage by poisoning the catalyst, which greatly reduces its electrocatalytic efficiency [28]. Currently, the most commonly used catalysts are noble metals such as Platinum and its alloys. The high cost and rareness in quantity make it a less-suitable option for such a large scale operation. Numerous non-noble and cheap materials have been identified having capability to catalyze methanol oxidation reaction (MOR) with high efficacy.

2.2 Electrocatalyst for DMFC:

Various electrocatalysts for MOR in DMFC have been introduced which may be homogenous like coordination complexes or heterogeneous like metallic nanoparticles or Pt-alloys [29] [30]

2.2.1 Platinum Based Catalyst:

Platinum has shown remarkable properties as a catalyst for methanol oxidation. In fact, it is the only material that has been used as a catalyst for commercial DMFCs despite its scarcity and high cost. To address these issues, Platinum has been combined with other metals to enhance the conductivity and reduce the cost. Among them, Ni, Cu, Co, Mo, Ti, Zn, Fe, Sn, Pd, and Ru etc. Platinum has also been attached to different Carbon containing compounds for example graphene, graphene oxide, and carbon nanotubes etc to assess its catalytic properties.

2.2.2 Platinum Based Alloy:

Platinum alone was firstly used as catalyst for MOR. The setup consisted of Mercury-Mercury oxide reference electrode and platinum mesh counter electrode. Two molar methanol solution was used in three different 0.5 Molar electrolyte solutions: NaOH, Na_2CO_3, $NaHCO_3$. The testing was conducted using a scan rate of 20mV/s. The test having 0.5M NaOH electrolyte showed highest current density of 3.8mA/cm^2 at -0.8V. 0.5M Na_2CO_3 electrolyte produced a current density of

1.9mA/cm^2 at -0.73V while $NaHCO_3$ generated a current density 1.8mA/cm^2. The research aslo concluded that alkali solutions perform well as compared to acidic solutions as they prevent Methanol crossover [29]. To enhance the electrochemical performance of Platinum, it was used in the form of nanoparticles with Ru and Mo. The Pt-Ru-Mo nanoparticles were synthesized using Bonnemann's method. The tests were conducted in 0.5M $H2SO_4$ solution with reverse Hydrogen electrode (RHE) as reference electrode, Platinum foil as counter electrode and Carbon rod as working electrode. The cyclic voltammetry curves show a peak current density of 2.5mA/cm^2 at 0.15V when the ratio of Pt-Ru-Mo was 1:1:0.5 [31]. Platinum deposited on Au nanoparticles possessed good catalytic capability for methanol oxidation reaction. The experiment was conduction in 2M methanol and 1M sulfuric acid solution. Reference electrode (RE) utilized was saturated calomel electrode (SCE) and working electrode was made of graphite. Two current peaks appeared at 0.48V and 0.6V with a peak current density of 402.2µA/cm^2 [32].

2.2.3 Platinum/Metal Oxide based Catalyst:

In [33], Pt-NiO alloy was burnt with carbon at various temperatures to prepare Pt-NiO/C alloys nanoparticles and results were compared with Pt/C. The results of cyclic voltammetry show that the synthesized material at highest temperature has highest current density as compared to others i.e., 49.22mAcm^{-2} at 0.2 V. In [34], Pt with V2O5 as composite with carbon black was applied as catalyst for methanol oxidation reaction in Hg/HgCl as reference electrode at 50 mVs^{-1}. The system generated current density of 15 mAcm^{-2} at 0.4 V. In [35], Pt-TiO_2 was tested for MOR in 0.5 M H_2SO_4 with Ag/AgCl reference electrode at 50 mVs^{-1} producing 28 mAcm^{-2} current density at 0.3 V. Pt-RuO_2 was also implemented as electrocatalyst [36] in DMFC which ultimately showed a current density of 23.9 mAcm^{-1} at a potential of 0.5 V. In [37], Pt-WO_3 alloy based catalyst was also used for methanol oxidation reaction in DMFC which gave current density of 3.8 mAcm^{-2} at a potential value of 0.2 V in 0.5 M H_2SO_4 at 0.1 mV/s.

2.2.4 Nanotubes Based Electrocatalyst For MOR:

Multi-walled carbon nanotubes have been applied as hybrid with platinum nanoparticles as electrocatalyst for MOR. In [38], overall current density obtained was 15.1 mAmg^{-1} at 0.7 V, in [39], it is 49 mAcm^{-2} at 0.7 V while in [40], it is 8 mAcm^{-2}at 0.7 V. in 0.1 M H_2SO_4 at 20 mVs^{-1} with dynamic hydrogen electrode as reference electrode. Pt-Ni alloy with CNTs was also tested

for MOR in the same media as above which generated current density of 30 $mAcm^{-2}$ at 0.7 V [41]. In 2005, Pt/CNT nanowires were tested for the same purpose [42]. It generated current density of 1.55 $mAcm^{-2}$ at 0.7 V in 1 M H_2SO_4at 50 mV/s. In 2007, same material in the form of composite was tested again at different scan rate and generated a current density of 94 $mAmg^{-1}$ at 0.6 V in 1M H_2SO_4 [43].

2.2.5 Nanoparticles of Platinum-Metal Alloy based electrocatalysts for MOR:

Pt-Ru nanoparticles were applied as electrocatalysts in methanol oxidation reaction(MOR) in DMFC in 0.5 Molar H_2SO_4 against standard Colemol Electrode (SCE) [44]. This system generated current density of 11 mA/cm^2 at 0.7 V. Pt-Ni Nanoparticles were also tested in the same conditions at 60 mVs^{-1} [45] and it resulted into the current of 550 μA at 0.4 V in 1 Molar Sulfuric acid at 50 mVs^{-1} against SCE as reference electrode. Pt-Au Nanoparticles in 0.1 Molar Sulfuric acid at 20 mV/s gave 1.7 mA/cm^2 current density at 0.7 V in 2006 [46] while it was 10 $mAcm^{-2}$ at 50 mVs^{-1} in 2007 [47]. Nanoparticles of Pt-Pd alloy were investigated with 0.5 M H_2SO_4 at 50 mVs^{-1} for MOR and generated current density of 14 x 10^{-4} $mAcm^{-2}$ at 0.6 V. In the same system, Pt-Cu nanoparticles were also tested and overall current density generated was 680 mA per mg of Pt [48]. Solo Pt nanoparticles as hybrid with graphene were also tested in the same system as above for MOR and this resulted into current density of 2.2 mA/cm^2 at 0.6 V [49].

2.2.6 Graphene Based Electrocatalyst for Methanol Oxidation:

Graphite Nanoplate-Pt and GO-Pt composites were tested for MOR in DMFC as electrocatalysts against SCE as reference electrode in 1M H_2SO_4 at 20 mVs^{-1} and resulted in current density of 47.5 $mAcm^{-2}$ and 52.1 $mAcm^{-2}$ respectively [50]. Pt-SiO_2-G composites with different concentration of tetraethyl orthosilicate (TEOS) were prepared and electrochemically analyst as catalyst for MOR in DMFC [51]. Among them one with greatest concentration of TEOS showed highest current per mg of Pt i.e., 1010 mA per mg of Pt at 50 mVs^{-1} in 0.5 M H_2SO_4 against Ag/AgCl reference electrode. Other composite catalysts in the same work resulted in current of 313 mA and 483 mA per mg Pt whereas sole Pt-G composite generated current of 225 mA per mg Pt at same conditions. Pd/Polypropylene as composite with graphene generated current density of 359.8 $Ag^{-1}$of Palladium at 0.2 V in 0.5 M NaOH at 50 mVs^{-1} [52]. Pt-Ru/G composite generated 19 $mAcm^{-2}$ current density

at 0.4 V in 0.5 M H_2SO_4 at 50 mVs^{-1} whereas Pt/G generated 20 $mAcm^{-2}$ current density in the same conditions [53]. Pt/GO composites generated 73 $mAmg^{-1}$ of Pt 0.7 V against Ag/AgCl reference electrode [54].

2.3 Metal Organic Framework for Energy Applications:

Metal organic framework are crystalline structures made by linking organic and inorganic units to the metal center which leads to various architectures with different properties like porosity. Metal organic framework normally yields tremendous porous structure having great thermal strength and chemical stability but we can alter these properties by switching from one linker to the other. Generally a MOF has about 50% of its volume free and available [55]. Initially, MOFs were called coordination polymer due to having similar structure but they are not as discrete as coordination polymers use to be. Later on in 1995[56], they were named metal organic frameworks (MOF) and thus are now considered a separate class of compounds. Due to having long sized linkers (usually organic) connected to metals, they have large voids left blank within the molecular structure. These spaces were studied thoroughly for the first time by compelling gas molecules into these voids at high pressure [57]. However the permanent porosity was analyzed and proved to be existing by testing the measurement of carbon dioxide and nitrogen isotherms on zinc based terephthalate MOF [58]. If we look deeply into the pore apertures, these are large enough, upto 2 nm, to accommodate small sized molecules but this property is not limited until here. We could alter the pore size and the suitable way to do so is to use long rod-shaped subunits as linkers. It provides periodicity to the other two dimensions as well and the structure in all the three dimensions doesn't allow interpenetrating of neighboring structures keeping almost all of the volume available for storage and enhances surface area for particular applications.

2.3.1 Gas Storage:

Current interests towards MOF applications also include its usage in fuel gas storage for example hydrogen, methane, methanol etc. this was first reported in 2003 for MOF-5 structures 31 [59]. Enhancing the volume of the pore and positively changing the surface area markedly increases the gas uptake at high pressure and 77 K temperature. For example NU-100 and MOF-210 both

exhibited gas uptake as high as 9.0 weight percent at 56 bar [60]. Mercedes-Benz have developed MOF based hydrogen fuel tanks in one of their model with fuel-cell power.

2.3.2 Carbon Dioxide Capturing:

MOFs also offer reversible adsorption of CO_2 within the porous structure. This application was initially published in 1998 for MOF-2. In 2005, further study of CO_2 capturing was done in MOF-177 which had uptake capacity of 1470 mg/g at 35 bar pressure. The best carbon dioxide uptake is reported to be 2437 mg/g at 50 bar in MOF-200. This illustrates that a gas container loaded up with MOF-200 or MOF-177 will accumulate carbon dioxide 9 times as much as stored in the same tank without containing MOF.

2.3.3 Proton Conductivity for Fuel Cell Applications:

A novel horizon in MOF research in MOF studies is about its application in fuel cell as proton conducting membrane [61]. Among the first ones to be tested and reported is MIL-53 MOF with acidic functionalization necessary for enhancing conductivity [62]. Later on, some MOFs with acidic functionalization or protein addition as proto carrier showed a better proton conductivity [63]. Extensive research is done over polymeric membranes e.g. that with perflourosulfonic acid (Nafion) is highly studied and applied polymer electrolyte membrane but such a membrane is highly expensive and also faces some problems regarding operating temperature and humidity [64]. So, MOFs can be an attractive alternative to this problem with an offer of tunable ultrahigh porosity, functionality and stability.

2.3.4 MOF Nanocrystals:

A completely new trend towards MOF synthesis approach is making its nanocrystals. By means of diverse synthetic approaches, the overall size, crystallinity and topography of the MOF can be controlled accurately [65]. The first attempt towards this achievement is in 2003 where MOF-5 crystals were synthesized at room temperature with crystal size of about 70-90 nm [66]. ZIF is also included in this run, whose crystals were made in nano size at room temperature. The whole mechanism illustrated later explained that the nucleation process was slow at first but got fast later

on leading to the synthesis of nano sized crystals [67]. Anyhow, this leaded to extensive properties of MOF and promising applications. The formation of nanocrystals, their assembling to make bigger structures and their integration into the electronic and chemical system devices are the most recent research interests.

2.3.5 Catalytic Activity of MOF:

Tunable pore metrics, and enhanced surface area within the open structures of MOFs leads to many advantageous applications towards catalysis. MOFs can act as capsulated catalysts within their pores [68]. For the very first time, MOFs were applied as catalyst in 1994, where Cd based metal organic framework with bipyridyl was used as linker was used for cyanosilylation of aldehydes [69]. MOF has also been implemented as heterogeneous catalyst. One early example for this case is that of *PIZA-3* [Mn_2 $(TpCPP)_2$ Mn_3] consisting of metalloporphyrin which was used for epoxidation of olefins [70]. Currently, MOF is being used as catalyst for various catalytic purposes i.e., oxygen reduction reaction (ORR), hydrogen evolution reaction (HER) and oxygen evolution reaction (OER) via water splitting [71], hydrogen oxidation reaction (HOR) and methanol oxidation reaction (MOR). Moreover, integration of nanomaterial with MOF for catalysis was carried out via post-synthetic modification (PSM) to enhance particle stability and to generate uniform pore distribution [72].

2.4 Areas Unexplored:

The thorough study of research work done until now for the betterment of DMFC activity and stability opens many new routes as well. From the literature, we can see that there are still some fields through which we can expand the studies and research. Some of the areas unexplored until now are;

- No work has been done with catalyst without containing Pt as a component for DMFC.
- Metal organic framework has never been tested for MOR in DMFC
- Composites with GO have been tested for evolution reactions and reduction reactions but they are not been used for methanol oxidation purposes
- Very less effort has been done to improve the values of potential or voltage towards lower values.

CHAPTER 3

Experimentation

3.1 Synthesis of Catalysts

The chemicals used in the synthesis procedure were bought from Sigma Aldrich in pure form and did not undergo any further modification and were used in ‘’as it is’’ condition. Chemicals used were; Copper nitrate hexahydrate ($CuNO_3.6H_2O$), trimesic acid (benzene tricarboxylic acid), double deionized water, N,N-dimethylformamide(DMF), graphite flakes, triethylamine (TEA), conc. sulfuric acid (H_2SO_4), potassium permanganate($KMnO_4$), and hydrogen peroxide (H_2O_2).

3.1.1 Synthesis Of Cu-BTC:

CU-BTC was synthesized through an easy hydrothermal method[73]. Trimesic acid (1,3,5-Benzene Tricarboxylic acid) was taken in 1.5g amount and was mixed through stirring in a 45mL mixture of equal quantity of Ethanol and N,N, Dimethyl Formamide. Another mixture was prepared by diffusing 3.114g of Copper Nitrate Hexahydrate in 22.5mL of double deionized water. The two solutions were mixed together through stirring for a period of ten minutes and then put into Teflon-lined autoclave for heating. The heating process was carried out at 100C for 10 hours. After that the sample was washed via vacuum filtration with Methanol for numerous times. The washed material was then dried in vacuum at 60C for 10 hours. The culminated sample was further used for desired application.

3.1.2 Synthesis of Graphene Oxide:

Graphene Oxide was prepared via Improved Hummer’s method[74]. 3g of Graphite flakes were dissolved in a 400mL liquid mixture of Sulfuric acid and Phosphoric acid in a ratio of 9:1. Later on , 18g of $KMnO_4$ was added into the solution that initiated the first oxidation round which resulted in a slightly exothermic reaction. The mixture was kept at a temperature of 323K with continuous stirring for ten hours. The stirring was followed by addition of 400mL of freezing water to start the second round of oxidation process which was stopped later by the addition of H_2O_2. The solution was then allowed to settle for 24hr and then it was filtered with HCl, Methanol and deionized water for numerous

times until the Ph of the solution reached normal. The washed solution was then dried at 333K and then was used for further applications.

3.1.3 Synthesis of Composites of GO/Cu-BTC:

The hybrids were formed through the same method as used for pure mof. 1.5g of 1,3,5-Benzene Tricarboxylate was mixed in 45mL mixture of equal quantities of Ethanol and DMF. Another solution was prepared by Copper Nitrate Hexahydrate in 22.5mL of deionized water which was then allowed to mix up. Graphene Oxide was added to the same solution according to the concentration specified by the composite. The two solutions were mixed and homogenized through stirring and sonication. The final solution was added into high pressure autoclave having Teflon lining and subjected to heating at 100C for 12 hours. The resulting material was washed through vacuum filtration with Methanol and Ethanol for numerous times. The agglomerated powder was heated in vacuum oven at a temperature of 60C for 10 hours. The final composite was saved in air tight vial.

3.2 Electrochemical Set up

The electrochemical behavior of the material was tested using cyclic voltammetry (CV) in 1M NaOH and 3M methanol Solution. The oxidation of Methanol was conducted in a system having three electrodes. Reference electrode is fixed potential electrode which provides voltage to the working electrode to initiate and progress the reaction. Counter electrode, which is also known as auxillery electrode collects the current from working electrode. It is used to complete the circuit.

3.2.1 Modification of working electrode (GCE)

For electrochemical measurements, a specific amount of the catalyst material i.e., 2 mg, 20μL Nafion solution and 80μL of ethanol were combined to form catalyst ink. This solution was thoroughly stirred to make proper binding and complete dispersion between the Nafion and the catalyst material. After that the 15 μL of the mixture was deposited carefully over the electrode surface using micropipette.The electrode surface was dried to make the thin film over it before starting up the electrochemical measurements. The catalytic characteristics were investigated with varying concentration of catalyst at fixed scan rate and with same concentration but changing the scan rates. The effect of Methanol concentration was also studied.

CHAPTER 4

Results And Discussions

4.1 Sample Characterization

The sample was characterized by XRD and SEM for its morphological studies, FTIR for determining the functional groups present, while the electrochemical properties were studied by CV and EIS and chronoamperometry.

4.1.1 X-ray Diffraction Pattern

The x-ray diffraction was done using X-ray powder diffractometer (XRD STOE θ-θ Germ Germany). 2θ values at 6.56o, 9.32, 11.5, 13.28, 18.92 at the position of (200), (220), (222), (400), (440) respectively exhibit the presence of Copper. The peak for GO is not prominent here because it was suppressed by the peak at 2θ of 10.92. Thus, Cu-BTC was perfectly added into the sheets of GO. The sole purpose of adding GO is to provide enhanced conduction properties. Moreover, this provides enhanced surface area for better catalytic activity.

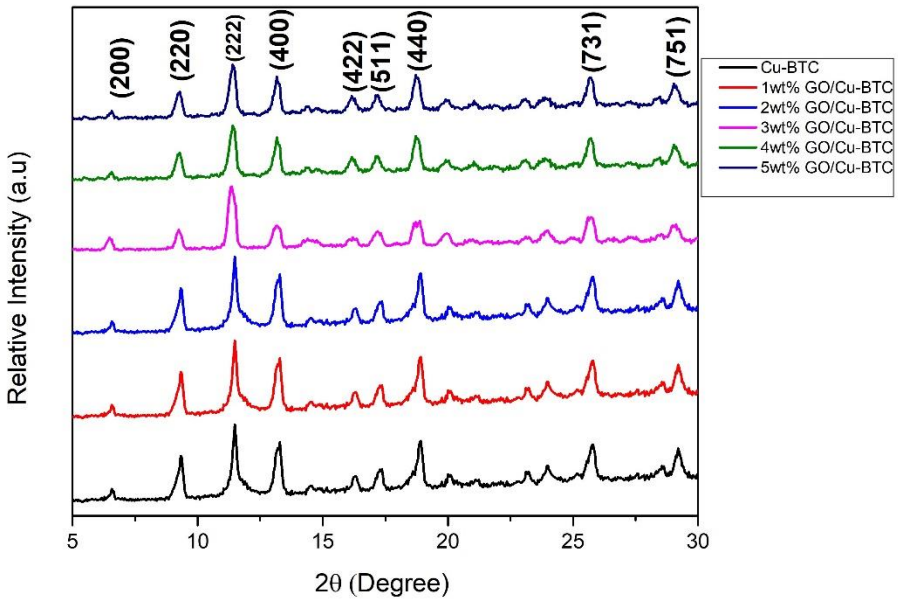

Figure 12: XRD pattern of Cu-BTC and composites with GO

4.1.2 Scanning Electron Microscopy

The morphology of synthesized material was investigated through scanning electron microscopy (SEM) using JEOL JSX-3201M and voltage was kept 10 KV. The pictures clearly indicate the incorporated CU-BTC cubes within the sheets of GO. The shape and fineness of the synthesized structure is a proof to the successful synthesis of Copper based Cu-BTC. In (b), the synthesis of GO layers can be seen clearly. The wrinkles visible in this particular SEM image are a clear evidence to the incorporation of GO. Furthermore, the SEM images of Cu-CU-BTC composites with 1-5 wt% GO (d) are shown. We can see that cubes of Cu-BTC are successfully incorporated over the surface of GO resulting into the preparation of composite with enhanced surface activity for better electrocatalytic results.

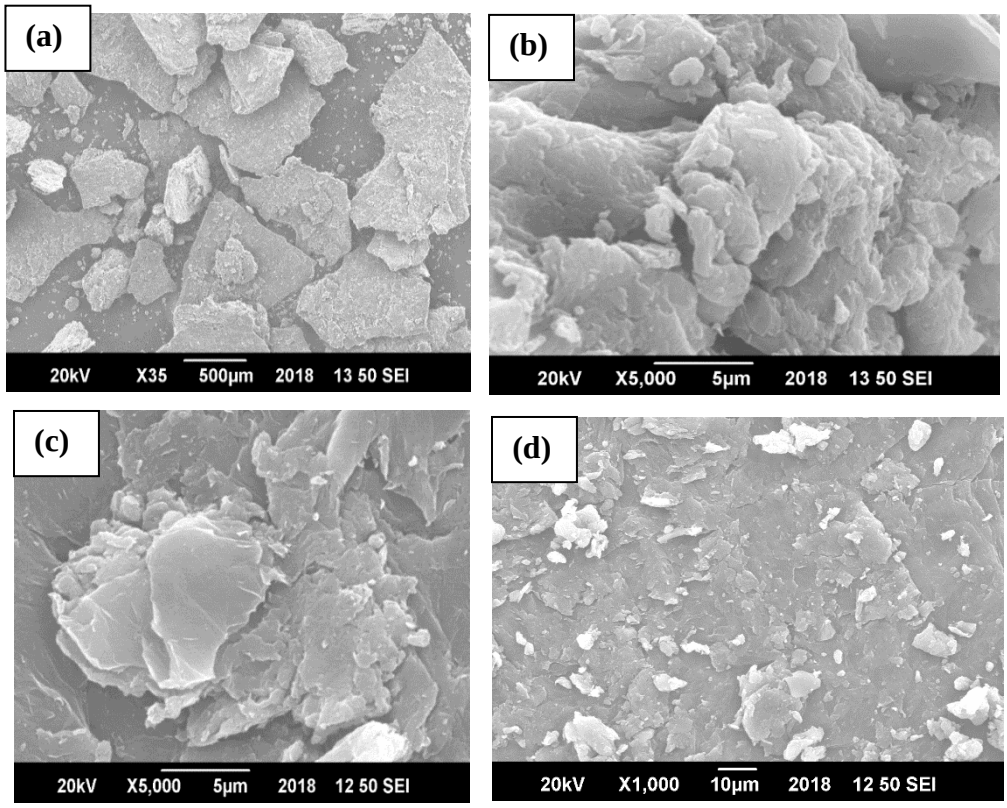

Figure 13: SEM images of GO

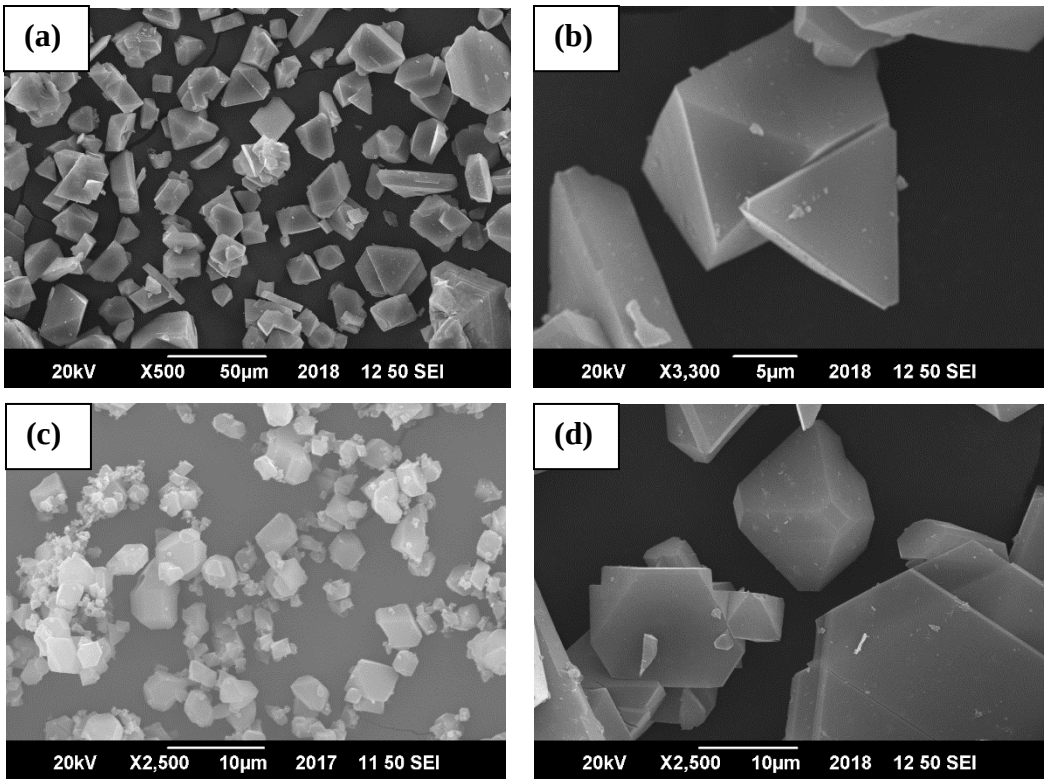

Figure 14: SEM images of Cu-BTC

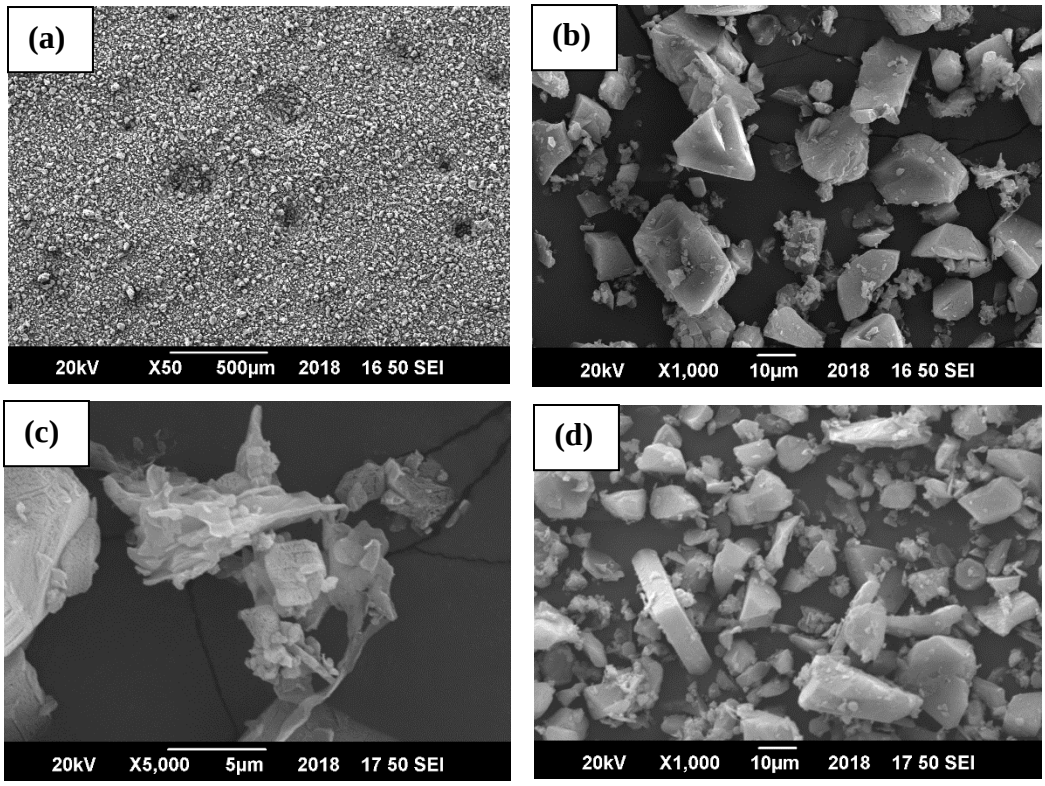

Figure 15: SEM images of Cu-BTC/1wt% GO

The SEM images of the 1wt% GO composites indicate clear octahedral structure of Metal Organic Frameworks crystals. The crystal's shape and size are uniform and well-defined which shows that controlled nucleation has taken place. Furthermore, Graphene Oxide sheets are seen wrapped around crystals and it can also be seen that the interaction of GO does not distort or disturb the orginal structure of MOF.

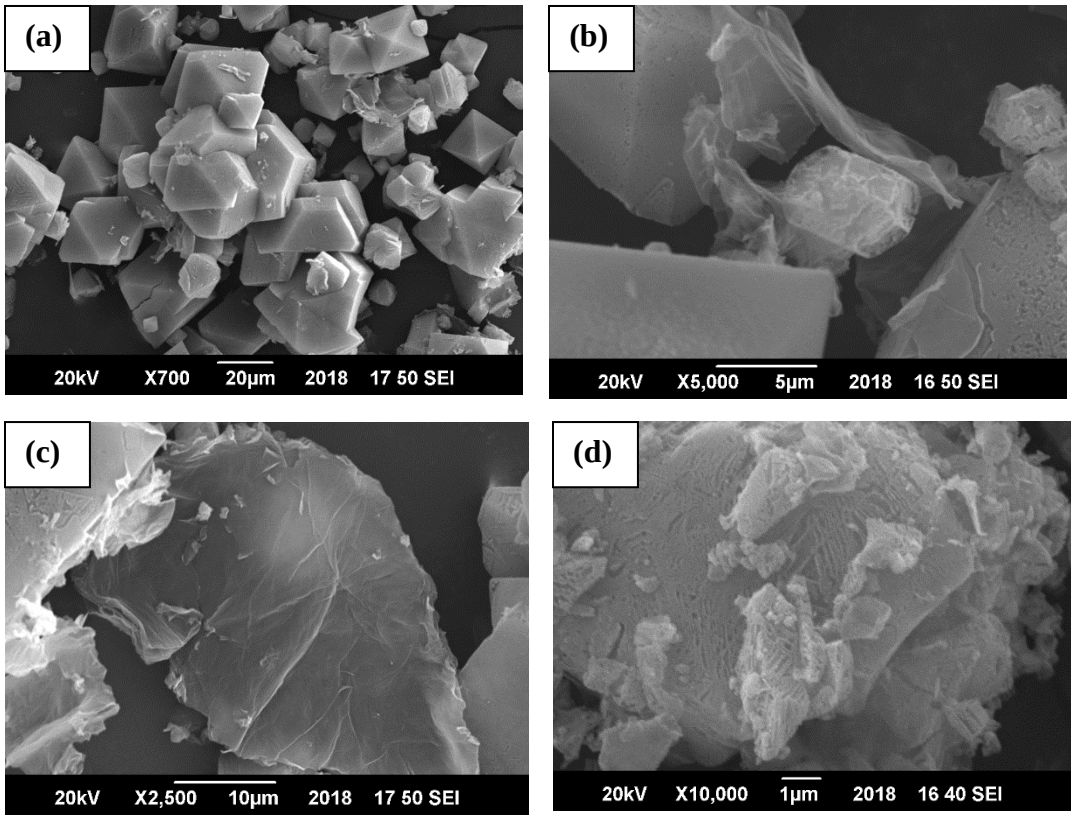

Figure 16: SEM images of Cu-BTC/2wt% GO

The SEM images of the 2wt% GO composites indicate clear octahedral structure of Metal Organic Frameworks crystals, Graphene Oxide sheets are seen wrapped around crystals and it can also be seen that the interaction of GO does not distort or disturb the orginal structure of MOF. Furthermore the crystal's shape and size are uniform and well-defined which shows that controlled nucleation has taken place.

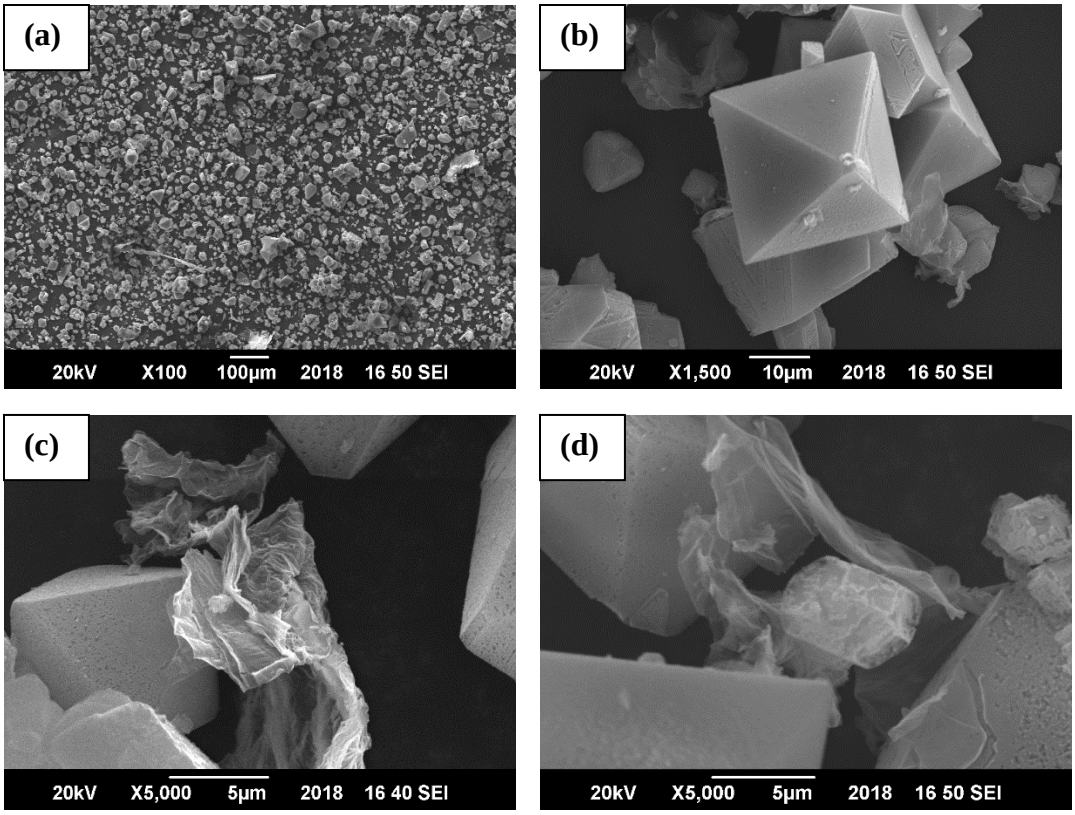

Figure 17: SEM images of Cu-BTC/3wt% GO

The SEM images of the 3wt% GO composites indicate clear octahedral structure of Metal Organic Frameworks crystals. The crystal's shape and size are uniform and well-defined which shows that controlled nucleation has taken place. Furthermore, Graphene Oxide sheets are seen wrapped around crystals and it can also be seen that the interaction of GO does not distort or disturb the orginal structure of MOF. The size has been found to vary with variations in temperature and concentration of reaction mixture. The perfect dispersion of CU-BTC and GO can be attributed to sonication at the time of synthesis. Furthermore, the crystal structure of MOF remained well-preserved with the incorporation of GO as illustrated by XRD. The shape and morphology of the synthesized MOF is quite similar to the previous reported data. The morphology of the structure has remained the same in all the samples, showing good reproducibility and consistency.

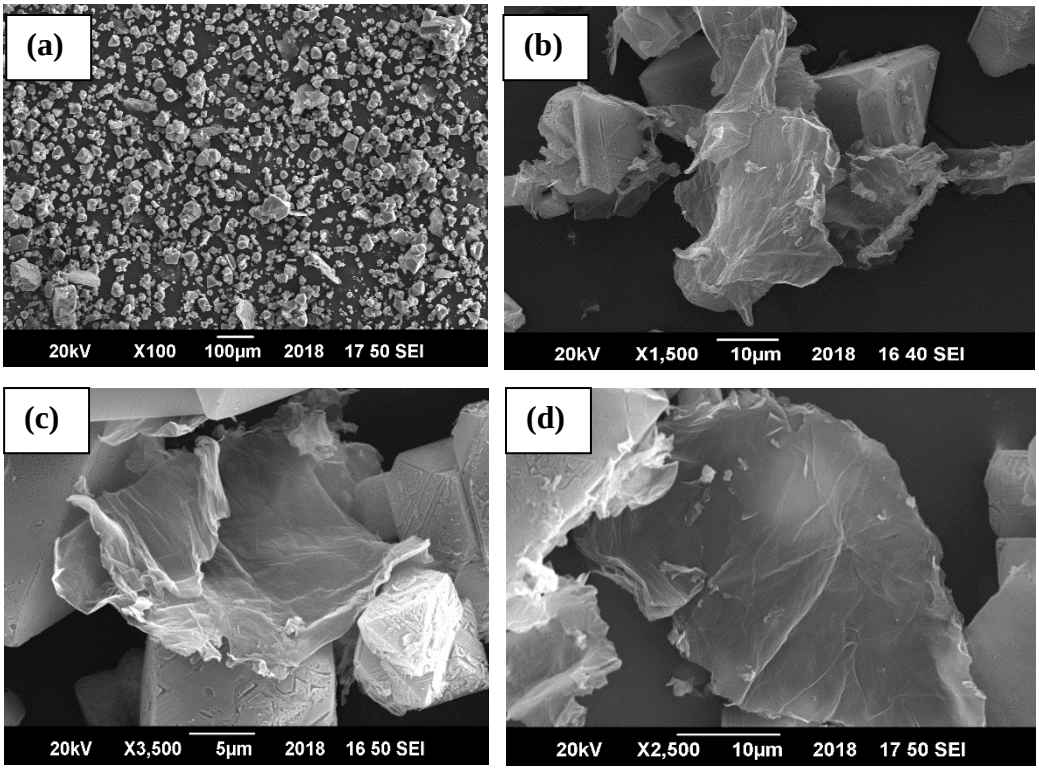

Figure 18: SEM images of Cu-BTC/4wt% GO

The SEM images of the 3wt% GO composites indicate clear octahedral structure of Metal Organic Frameworks crystals. The crystal's shape and size are uniform and well-defined which shows that controlled nucleation has taken place. Furthermore, Graphene Oxide sheets are seen wrapped around crystals and it can also be seen that the interaction of GO does not distort or disturb the orginal structure of MOF. The size has been found to vary with variations in temperature and concentration of reaction mixture. The perfect dispersion of CU-BTC and GO can be attributed to sonication at the time of synthesis. Furthermore, the crystal structure of MOF remained well-preserved with the incorporation of GO as illustrated by XRD. The shape and morphology of the synthesized MOF is quite similar to the previous reported data. The morphology of the structure has remained the same in all the samples, showing good reproducibility and consistency. The undisturbed morphology of crystals may signals at the type of bonding between the MOF structure and GO layers.

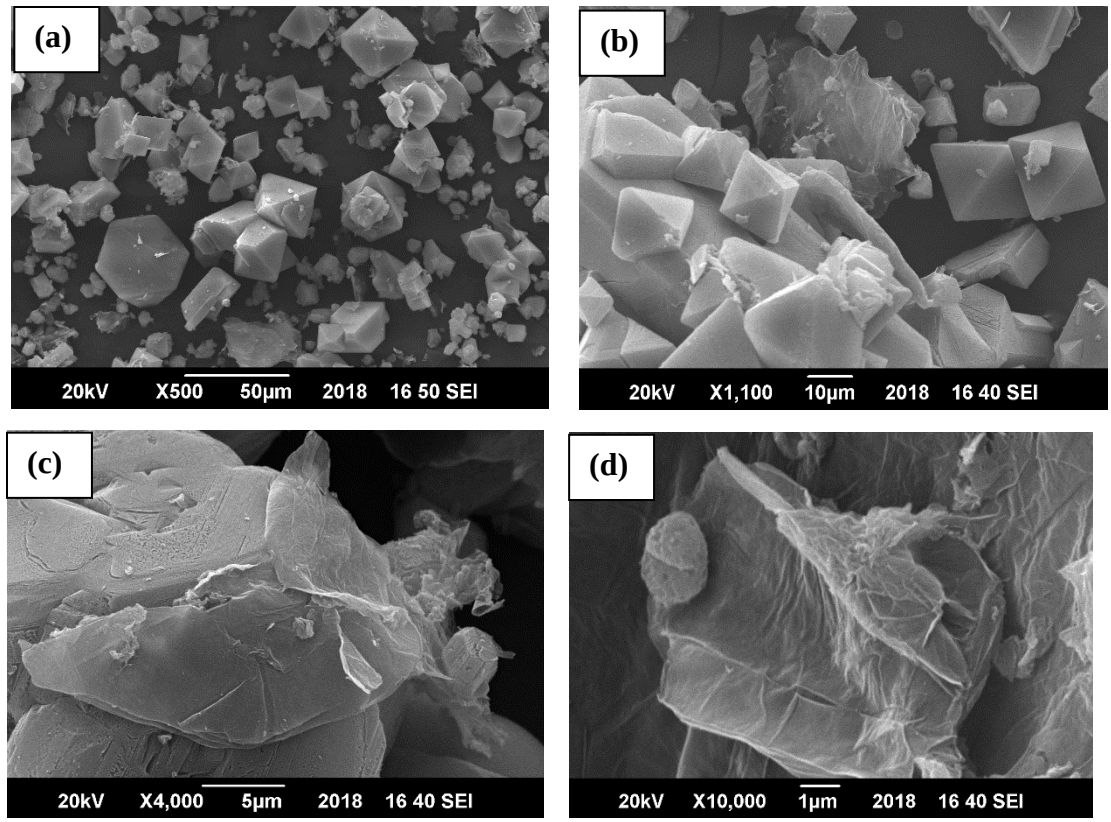

Figure 19: SEM images of Cu-BTC/ 5wt% GO

The SEM images of the 3wt% GO composites indicate clear octahedral structure of Metal Organic Frameworks crystals. The crystal's shape and size are uniform and well-defined which shows that controlled nucleation has taken place. Furthermore, Graphene Oxide sheets are seen wrapped around crystals and it can also be seen that the interaction of GO does not distort or disturb the orginal structure of MOF. The size has been found to vary with variations in temperature and concentration of reaction mixture. The perfect dispersion of CU-BTC and GO can be attributed to sonication at the time of synthesis. Furthermore, the crystal structure of MOF remained well-preserved with the incorporation of GO as illustrated by XRD. The shape and morphology of the synthesized MOF is quite similar to the previous reported data. The morphology of the structure has remained the same in all the samples, showing good reproducibility and consistency. The undisturbed morphology of crystals may signals at the type of bonding between the MOF structure and GO layers.

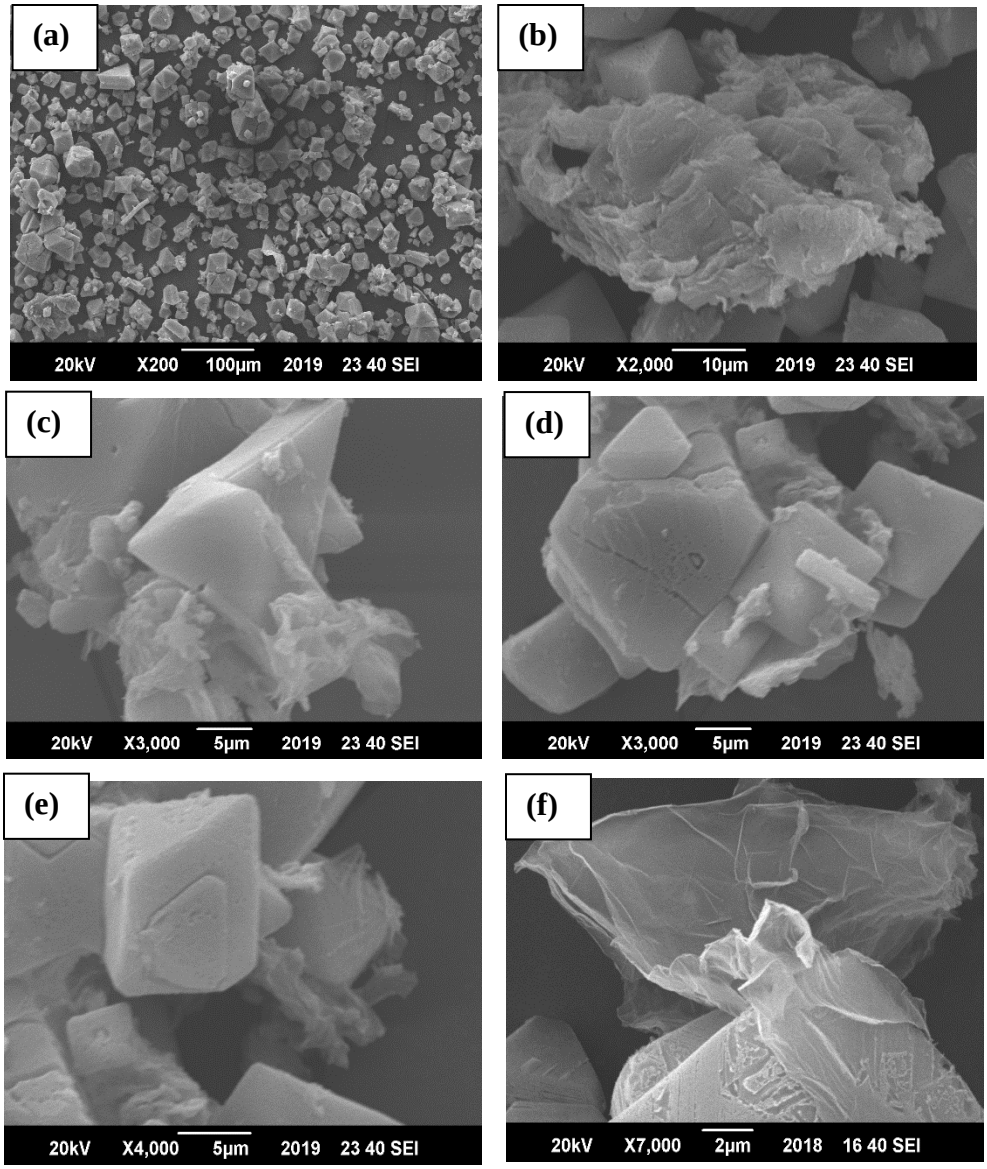

Figure 20: SEM images of Cu-BTC/8wt% GO

The SEM images of Cu-BTC/8wt% GO shows that although the original symmetry of the MOF crystals has been retained, the high concentration of Graphene Oxide has covered the surface of the crystals and blocked the pores of the MOF. This blockage can become a hurdle in the way of electroactive species to reach catalytic active sites and thus hinder the catalysis process. Thus the current density of this sample as found by cyclic volametry technique is quite lower than the sample containing 5wt% GO. Therefore, we have optimized the concentration of GO for making composites with C-BTC in this way.

4.1.3 Fourier Transform Infrared Spectroscopy:

Infrared spectra of the materials also gives a clear indication of functional groups that should be present in the material. The sleek peak at 1590 cm^{-1} signals the existence of carboxyl functional group in all the materials while the appearance of small bell-shaped region at around 36000 cm^{-1} is evidence to the presence of GO in the composites. The carbonyl group is due to the presence Trimesic acid groups around the corners of cubical Cu-CU-BTC structure. The peak at 1448cm^{-1}

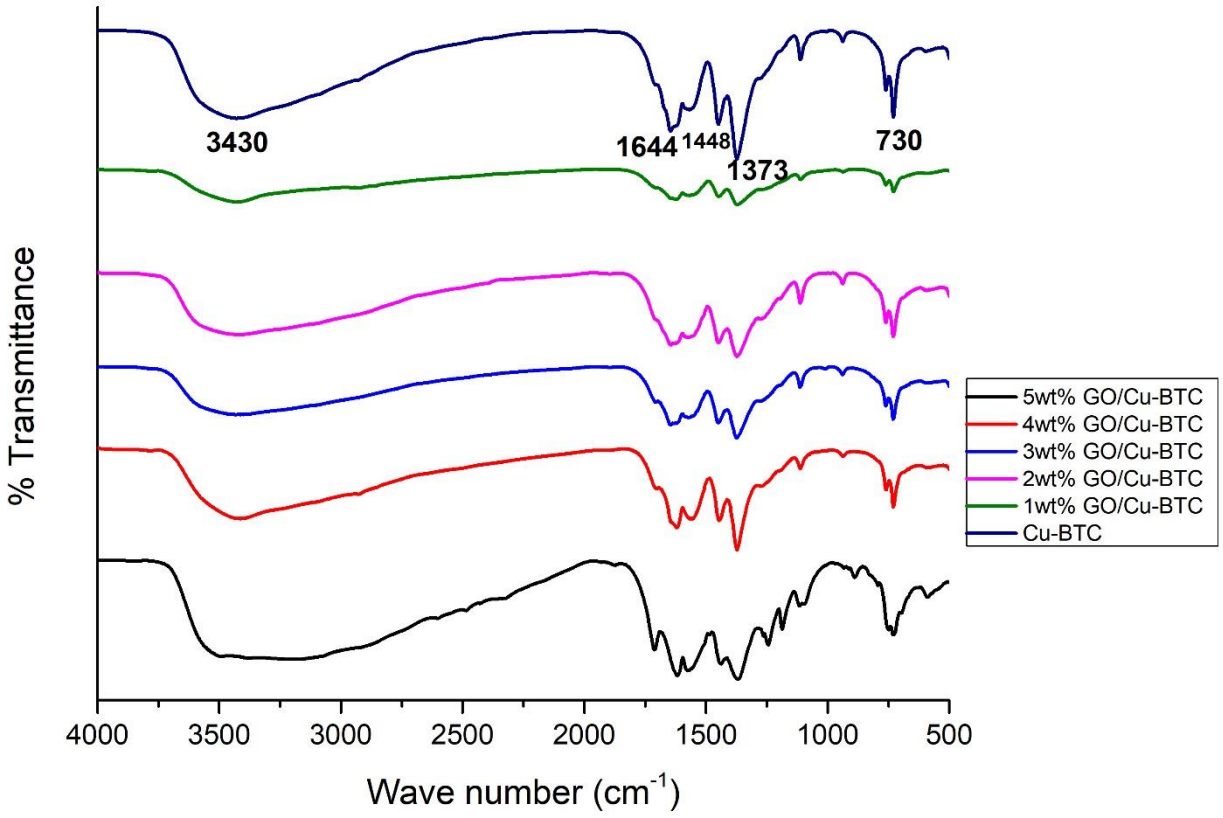

Figure 21: FTIR spectrum of Cu-BTC and (1-5)wt% GO/CU-BTC

indicates the presence of Benzene ring while the peak at 730cm^{-1} gives a clue about the Copper bonded to Oxygen, showing the linkage between Copper and the linker which is Trimesic acid.

4.2 Electrochemical Characterization:

All the electrochemical experiments were done using a three-electrode system containing 3M methanol solution as fuel and 1M NaOH as supporting electrolyte. The electrode used for this purpose was glassy carbon electrode (GCE). Nafion solution was used as an efficient binding agent. The scans were taken for both bare and modified GCE.

4.2.1 Cyclic Voltammetry:

The setup used for conducting the electrochemical studies was of GARMY G750 in potentiostatic mode. The electrochemical analysis started with a scan of bare GCE in 3 electrode system filled with 3M methanol and 1M NaOH. This results into the response of NaOH which acts as supporting electrode.

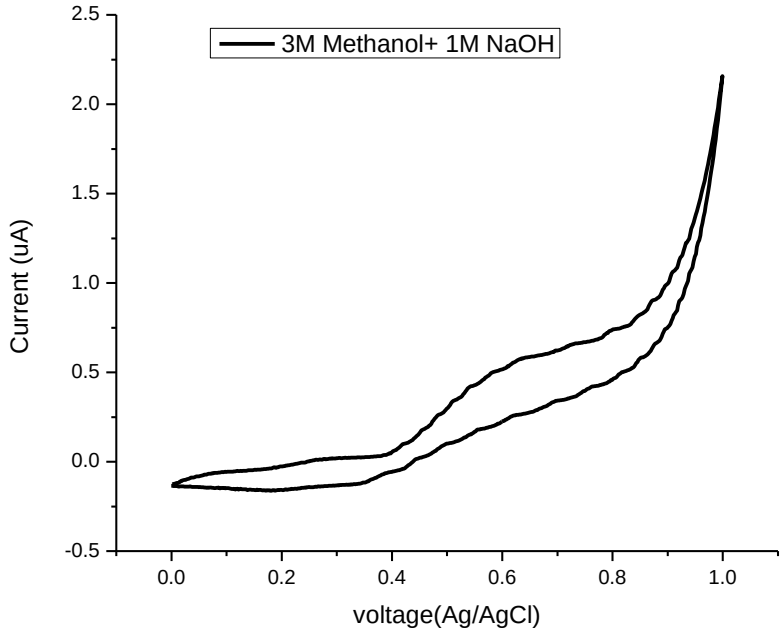

Figure 22: CV of bare electode.

The role of supporting electrode is quite significant. Normally a supporting electrode is a bulky group which helps controlling population of charged ions, protons in this case, at electrode. As a

result, the system counts a cluster of charged species per second giving off a reliable valuable of current density at a point of scan.

4.2.1.1 Effect of GO Concentration:

GCE was also modified by applying a thin layer of Cu-CU-BTC composite material with (1-5)wt% graphene oxide and the results were compared with that of Co-MOF-71 itself Fig. 4.6. The catalysts were taken in 2 mg concentration at scan rate of 50 mVs^{-1}. The comparative results in cyclic voltammetry for un-deposited and catalyzed electrode are to be taken to observe the change in response of the catalyst upon adding GO.

The outcome of adding Graphene Oxide to the MOF structure is tremendous and has huge impact on its performance. As the GO was added, the current shot up almost twofold. This is due to high electron conductive property of GO and its high surface area. The highest concentration of GO was optimized by inspecting catalytic properties of 8wt% sample. The current achieved with this sample was lower than that of 5wt% GO/Cu-BTC, which is probably due to the fact that such high concentrations of GO covers the pores of MOF, thus blocking active catalytic sites. The overall current density increased from 48mA/cm^2 to 147mA/cm^2 as the concentration of GO was increased from none to 5wt%.

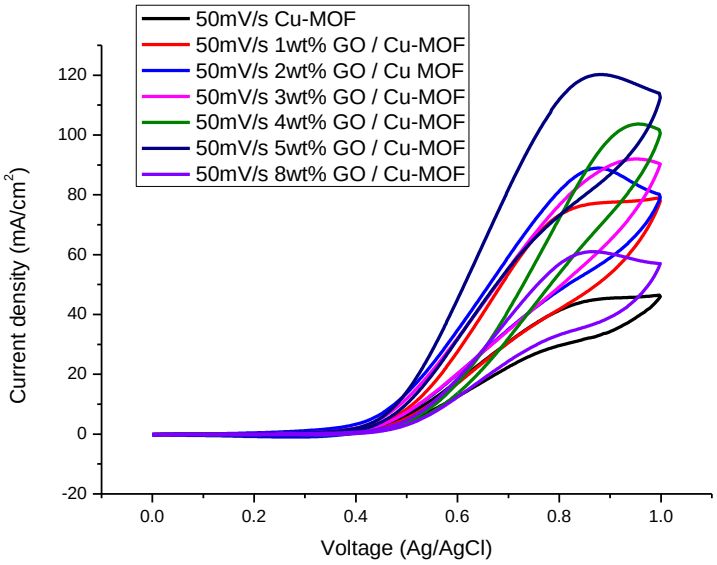

Figure 23: Comparison of CV results among different samples

This enhanced current density value of 5 wt. % GO composite clues at lesser activation energy for oxidation of methanol in the presence of GO layers due to enhancement in the conductivity of the system. As far as other two composites with 8 wt. % and 10 wt. % are concerned, the efficiency was not satisfactory and as expected. This is the point to ponder; increasing the GO concentration after a certain limit doesn't follow the trend and has a negative effect on overall current density. One possible reason behind this may be the clustering of GO leading towards blockage of space. Another reason may be the possible charge separation over the large surface of GO resulting into the accumulation of charges at one point rather than moving forward for conductivity.

4.2.2 Study of Effect of Scan Rate:

The effect of scan rate (mVs^{-1}) was also studied by analyzing the same material (2 mg) at different scan rates i.e., 50 mV/s, 60 mVs^{-1}, 70 mV/s, 80mV/s, 90mV/s, and 100 mV/s for pure mof and (1-5)wt% GO/CU-BTC composites. Current has a direct relation with the square root of scan rate. The reasoning is as follows: current is dependent on concentration of Methanol on the electrode which in turn relies on the concentration gradient. The greater the concentration gradient, the lesser is the availability of Methanol on the surface and lesser will be the current. What scan rate does is it minimizes the diffusion layer, thus reducing the concentration gradient and enhancing the current.

Another reason of increasing the current density value with increase in scan rate is that at higher scan rates, only those species get oxidized or reduced that are electroactive. Thus, only those species make their way to the electrode surface that are capable of producing electrons.

The reason that why we have not gone above the scan rate of 200mV/s is because it leaves little time for the reaction to occur. There must be sufficient time for electroactive species to first diffuse from bulk solution to the electrode surface and then react at the electrode surface to get oxidized into products which in the case are carbon dioxide, electrons and protons at the anode. Therefore, there was no peak of methanol oxidation in voltammograms above scan rate of 200mV/s.

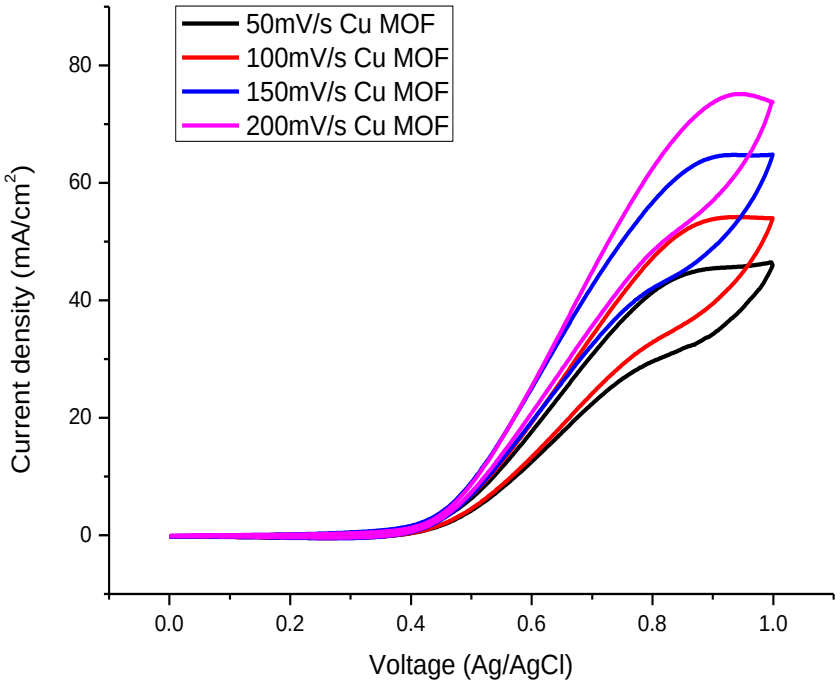

Figure 24: Effect of scan rate on current density of pure Cu-BTC.

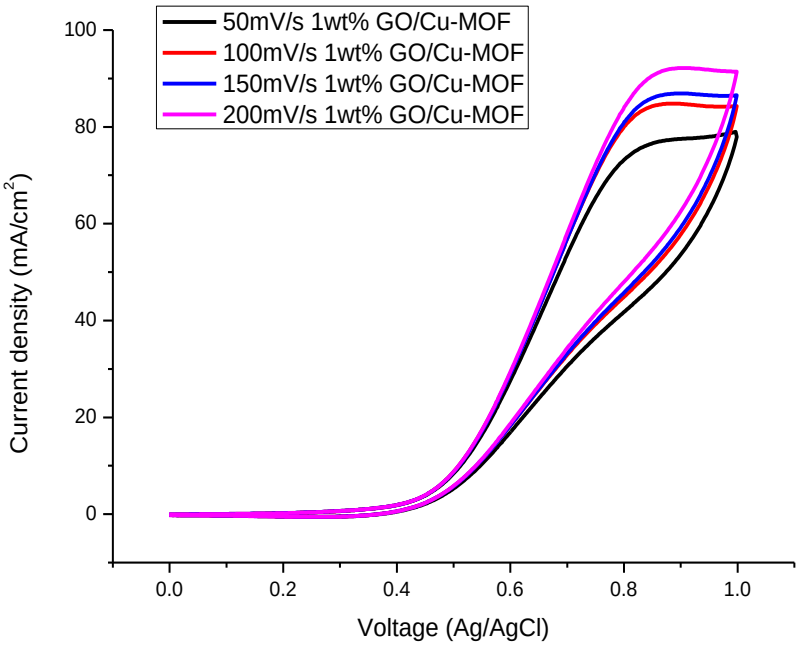

Figure 25: Effect of scan rate on current density of 1wt% GO/Cu-BTC

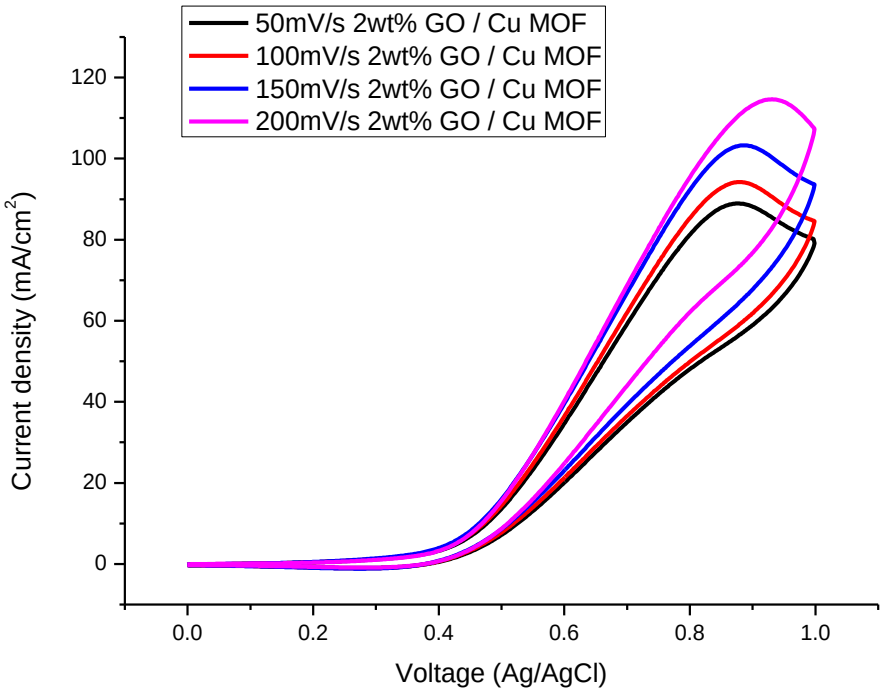

Figure 26: Effect of scan rate on current density of 2wt% GO/Cu-BTC

As the scan rate is increased from 100mV/s to 200mV/s, the current gradually enhances from 46.46mA/cm^2 to 62.61mA/cm^2, indicating the obeying of Randles-Sevick principle. Increased scan rate leads to depleted diffusion layer around the electrode which helps enhance the electrocatalytic activity by abetting the proton conduction across the electrolyte.

The impact of scan rate on current density is quite obvious. As the scan is increased from 100mV/s to 200mV/s, the current density has drastically hiked up with the same pace from 63.65mA/cm^2 to 112.24mA/cm^2 signifying the importance of scan rate. This is in complete accordance with Randles Sevick equation which state that current density is directly proportional to square rate of scan rate. This is due to the reason that Increased scan rate leads to depleted

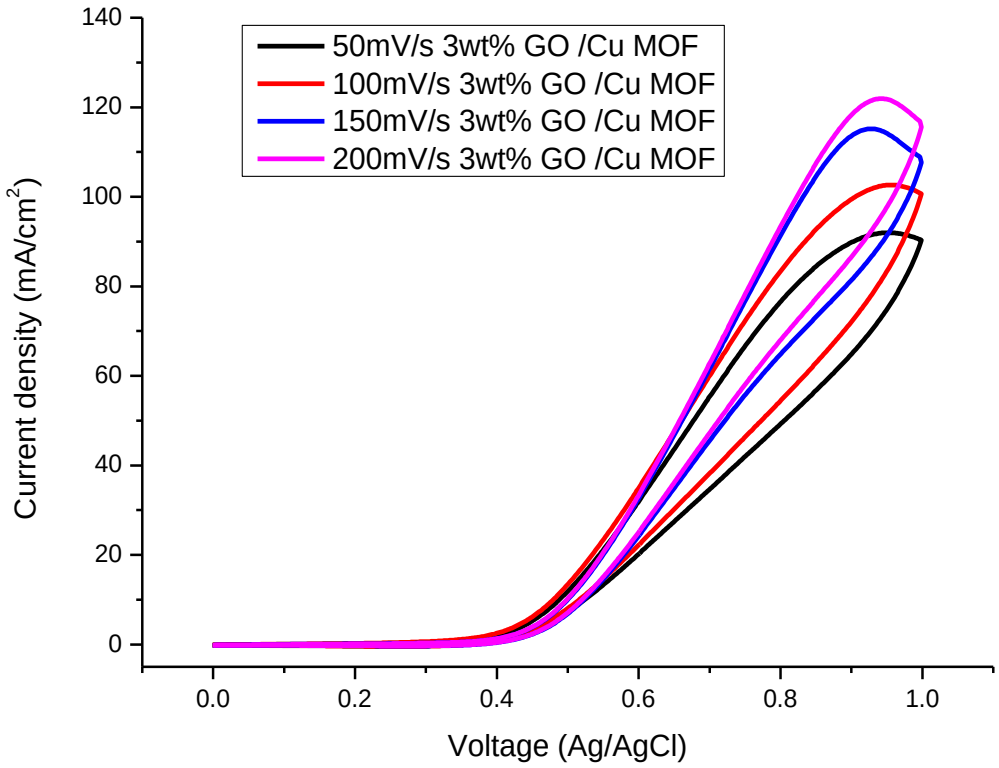

Figure 27: Effect of scan rate on cyclic voltammetry of 3wt% GO/MOF.

Diffusion layer around the electrode which helps enhance the electrocatalytic activity by abetting the proton conduction across the electrolyte. The variation of scan rate has a pretty blatant influence on cyclic voltammetric calculations. Increasing the scan rate from 50mV/s till 100mV/s, the current density has shot up accordingly from 73.14mA/cm^2 to 126.45mA/cm^2 indicating the following of Randles-Sevick equation which states the current density is directly linked to square root of scan rate. This is due to the reason that increased scan rate leads to depleted diffusion layer around the electrode which helps enhance the electrocatalytic activity by abetting the proton conduction across the electrolyte.

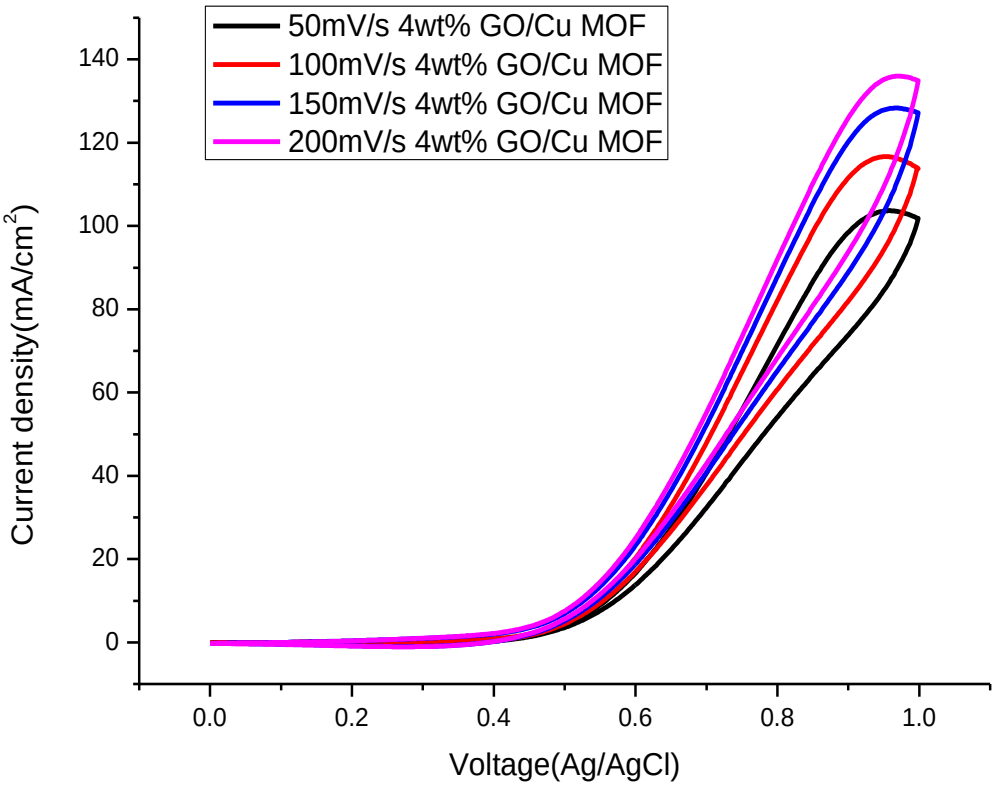

Figure 28: Effect of scan rate on current density of 4wt% GO/CU-BTC

The impact of scan rate on cyclic voltammetric graphs has been known since long. The above diagram depicts that when the scan rate is enhanced from 50mV/s till 200mV/s, the current density has gone up from 80.17mA/cm^2 to 139mA/cm^2 indicating the following of Randles-Sevick equation which states the current density is directly linked to square root of scan rate. This is due to the reason that increased scan rate leads to depleted concentration gradient around the electrode which helps enhance the electrocatalytic activity by abetting the proton conduction across the electrolyte. The increased concentration gradient is due to the high diffusion rates of electroactive species from the bulk solution of methanol to the electrode surface where they get oxidized or reduced to give carbon dioxide, electrons that travel through external circuit to reach cathode and protons that diffuse through electrolyte to reach cathode.

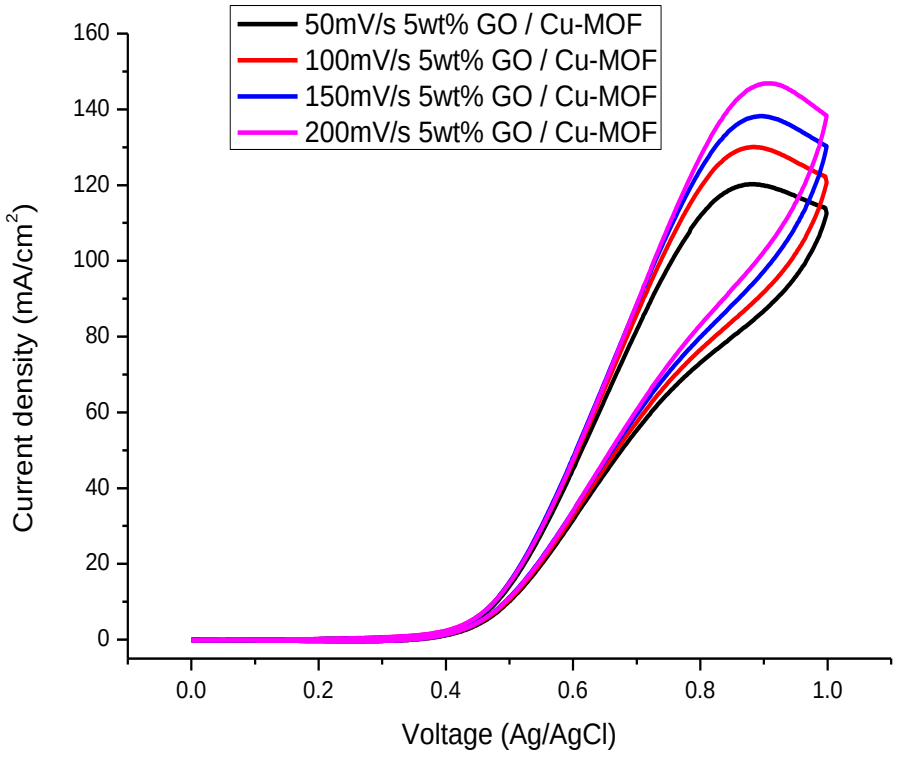

Figure 29: Effect of scan rate on cyclic voltammetric calculations of 5wt% GO/CU-BTC composites.

The impact of scan rate on cyclic voltammetric graphs has been known since long. The above diagram depicts that when the scan rate is enhanced from 50mV/s till 100mV/s, the current density has gone up from 80.17mA/cm^2 to 139mA/cm^2 indicating the following of Randles-Sevick equation which states the current density is directly linked to square root of scan rate. This is due to the reason that increased scan rate leads to depleted diffusion layer around the electrode which helps enhance the electrocatalytic activity by abetting the proton conduction across the electrolyte. The increased concentration gradient is due to the high diffusion rates of electroactive species from the bulk solution of methanol to the electrode surface where they get oxidized or reduced to give carbon dioxide, electrons that travel through external circuit to reach cathode and protons that diffuse through electrolyte to reach cathode.

4.3 Electrochemical Impedence Spectroscopy:

The electrochemical impedance spectroscopy (EIS) is an accurate method to inspect the performance of catalyzed electrode [98]. In EIS impedance is calculated using potentiostatic mode in the same three electrode system in 1M NaOH and 3M Methanol with un-deposited and modified GCE. EIS is usually represented by Nyquist plot or Bode plot. Nyquist plot consists of two axis. Y-axis being the imaginary one while the X-axis shows the real parameter because the formula for charge transfer resistance contains one coordinate that has imaginary number and the other one has real number.

Solution impedance to charge transfer is an important parameter for electrochemical studies. The resistance between reference and catalyzed working electrode must not be ignored wile computing electrochemical impedance of a circuit. By comparing the results, it can be seen that with increasing concentration of GO, the impedance faced by the charges gets lower. The plot between real and imaginary impedance is showing curves in low frequency area for modified GCE while with bare GCE it is just linear. The effect of different concentrations of CU-BTC on impedance was also studied. With increasing concentration of MOF, the impedance decreased allowing charges to pass swiftly without facing much resistance. This suggests that as the concentration of catalyst is increased the distance between catalyst layer and the electrode surface decreases. This allows the charge transfer to face lesser resistance towards diffusion.

The impedance studies were done with composites of Cu-BTC as well in which the effect of concentration of graphene was investigated over the overall impedance faced by the system. The comparative results show a huge decrease in the overall impedance clearly representing that the graphene has contributed towards ease of diffusion controlled mechanism of charge transfer. This also reflects that GO's property of conductivity has contributed towards the overall conductivity of the catalyst.

Solution resistance also plays a great role in diffusion of species from bulk solution to the electrode surface and must not be neglecting while calculating the overall resistance. Generally, the charge transfer resistance is calculated by measuring the radius of the incomplete semi-circle that is formed by Nyquist plot.

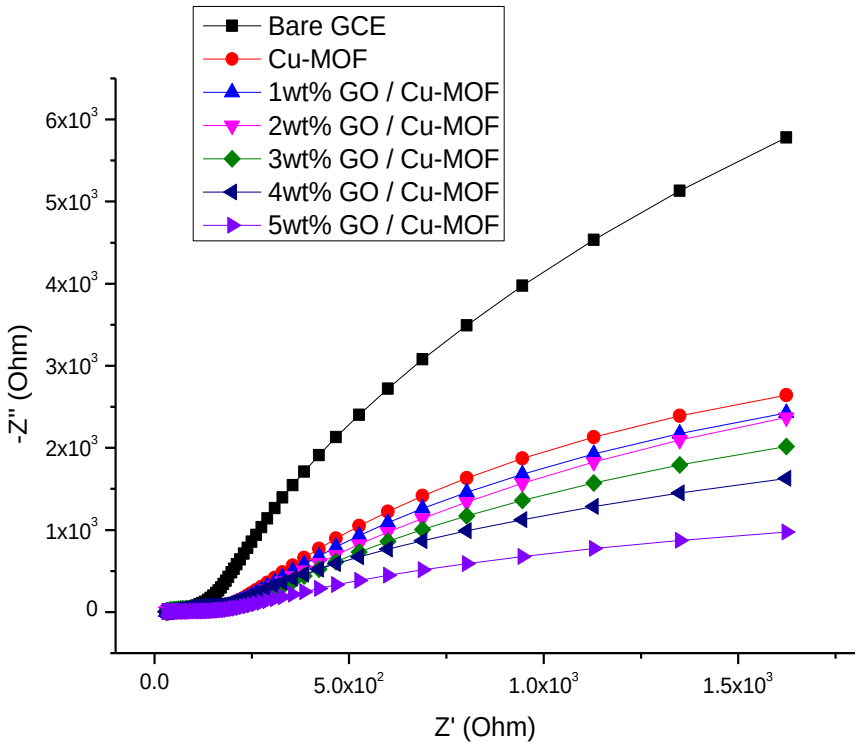

Figure 30: EIS graphs of different compositions of GO with Cu -BTC

As can be seen from the image above, it is evident that as the concentration of Graphene Oxide has increased, the charge transfer resistance has decreased accordingly. The reason is that the increased concentration of Graphene Oxide provides more surface area and more conductivity to the electroactive species, thus giving them more accessibility to the catalytically active sites which are Copper atoms, which are necessary for catalysis.

The comparative results show a huge decrease in the overall impedance clearly representing that the graphene has contributed towards ease of diffusion controlled mechanism of charge transfer. This also reflects that GO's property of conductivity has contributed towards the overall conductivity of the catalyst.

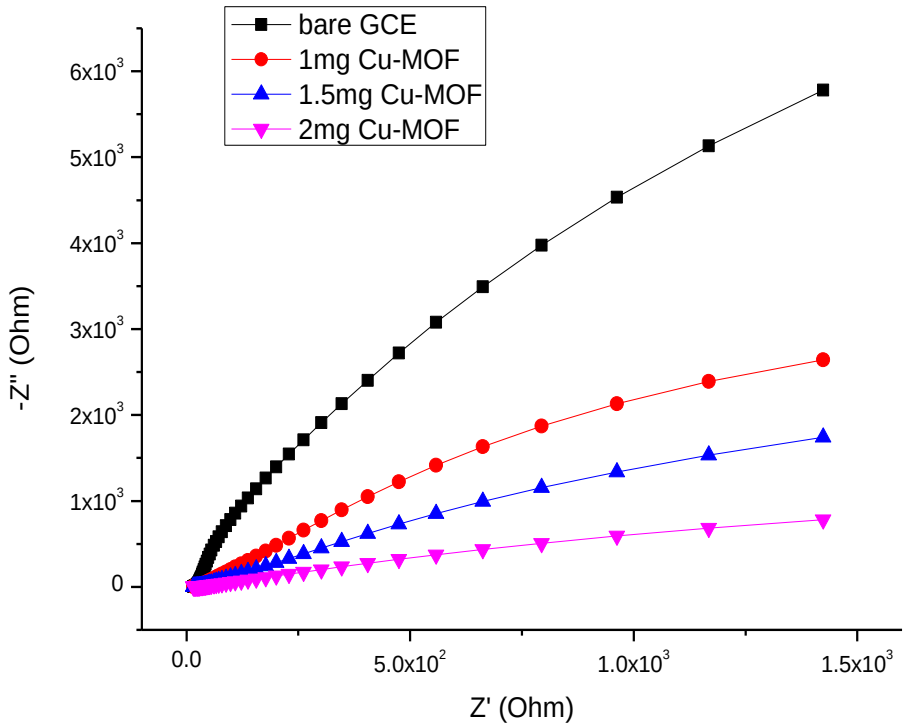

Figure 31: Nyquist plot for various catalyst concentration

The Nyquist plot for varying concentration of catalyst shows that as the concentration of catalyst of is increased, the charge transfer resistance for methanol oxidation reaction has decreased correspondingly. This effect goes to show that higher catalyst concentration provide greater catalytic area and easy access to catalytic active sites for electroactive species because the more the amount of catalyst, the greater will be the catalytic active sites and greater will be the surface area and conductivity of the material. In this catalyst, Copper atoms, which are the coordination centers, act as catalyst for Methanol oxidation reaction while the ligand of the MOF, which is Benzene Tricarboxylate and Graphene Oxide play the role of catalyst support to provide enhanced surface area and better conductivity.

4.4 Chronoamperometry:

To find the stability of the material during the catalytic process, chronoamperometry was carried out. The test was run for prolonged period of time of 3600s and voltage given was 0.8V. The initial drop in current density is well established and happens to every material but the point to focus on is how much current can the material retain for long period of time. The drop in current can be attributed to the blinding of pores by the methanol. At the start of the reaction, the pores are open but as the reaction proceeds, methanol takes up the space, limiting the reaction kinetics. The blinded pores with the passage of time, get cleared up as the reaction intermediates, which are responsible of clogging are reacted into final products and clears the path.

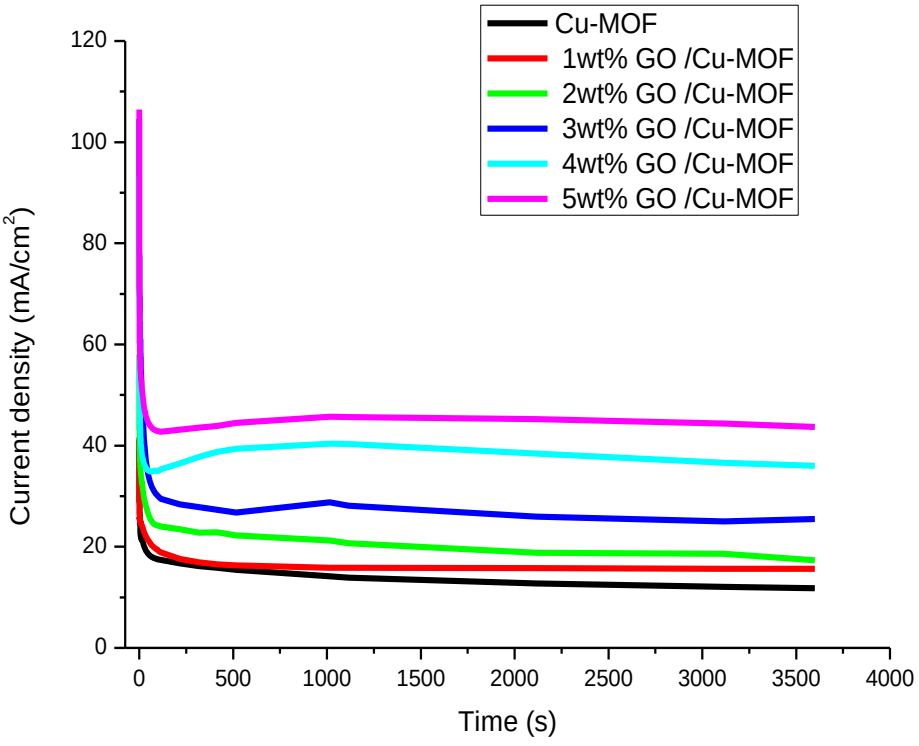

Figure 32: Chronoamperometric curves

Conclusion:

Cu-BTC MOF was synthesized via a facile hydrothermal method with high yield while Graphene Oxide was synthesized through Improved Hummer's method. The composites of MOF with (1-5) wt% of GO were also synthesized through hydrothermal method. Cu-BTC/8wt% GO was synthesized to optimize the concentration of GO. These samples were characterized through XRD, SEM, and FTIR.

XRD analysis shows that the material is highly crystalline and the incorporation of Graphene Oxide does not distort the actual structure of of Cu-BTC. SEM images visually display the cubical structure of MOF and it also shows wrapping of Graphene Oxide around MOF crystals. FTIR pattern revealed all the functional groups that come from Benzene Tricarboxylate and linkage between Copper and Benzene Tricarboxylate

Electrochemical properties of the synthesized catalysts were studied by cyclic voltammetry, electrochemical impedance spectroscopy and chronoamperometry with a three-electrode system with Ag/AgCl reference electrode, Pt wire as counter electrode and glassy carbon electrode as working electrode which was then scanned for methanol oxidation reaction both in bare and modified form. There has been observed huge difference in current density value between pure Cu-BTC and its composites with GO. The increase in current density value is attributed to high surface area and enhanced conductivity provided by GO which acts as a catalyst support. EIS results also show that the charge transfer resistance is significantly reduced by the addition of GO because of ease in the passage of electroactive species towards the catalyst while catalyst with high concentration of GO shows the highest stability for prolonged period of time. The resulting current density values on comparison with literature and standard value of platinum show that graphene has a positive impact over the porosity, surface activity and conductivity of the copper based MOF. So, we can say that Copper based structures and its nanocomposite using graphene oxide has an innovative role in electrochemistry especially in the field of MOR in direct methanol fuel cell (DMFC). Thus, these materials can be introduced as an alternate to the costly and poisoning Pt based catalysts.

Future Recommendations

- ✓ Effect of Platinum promotion on Cu BTC MOF can be tested for methanol oxidation reaction.
- ✓ The Cu-BTC GO composites can be studied for catalysis of Oxygen evolution reaction (OER).
- ✓ Effect of temperature on catalytic process of Methanol oxidation reaction.

References

[1] Adams, S., E.K.M. Klobodu, and A. Apio, *Renewable and non-renewable energy, regime type and economic growth.* Renewable Energy, 2018. **125**: p. 755-767.

[2] Hao Yu, E., K. Scott, and R.W. Reeve, *A study of the anodic oxidation of methanol on Pt in alkaline solutions.* Journal of Electroanalytical Chemistry, 2003. **547**(1): p. 17-24.

[3] ; Available from: B. Petroleum, "BP energy outlook 2035," BP stats, Jan, 2014.

[4] Wakeel, M., B. Chen, and S. Jahangir, *Overview of Energy Portfolio in Pakistan.* Energy Procedia, 2016. **88**: p. 71-75.

[5] Breeze, P., *Chapter 1 - An Introduction to Fuel Cells*, in *Fuel Cells*, P. Breeze, Editor. 2017, Academic Press. p. 1-10.

[6] Gong, W., et al., *Fast and accurate parameter extraction for different types of fuel cells with decomposition and nature-inspired optimization method.* Energy Conversion and Management, 2018. **174**: p. 913-921.

[7] A. K. Geim, and K. S. Novoselov. "The Rise of Graphene." Nature Materials, vol. 6, no. 3, 2007, pp. 183–191.

[8] Zhan, Z., et al., *Experimental study on different preheating methods for the cold-start of PEMFC stacks.* Energy, 2018. **162**: p. 1029-1040.

[9] Lin, B.Y.S., D.W. Kirk, and S.J. Thorpe, *Performance of alkaline fuel cells: A possible future energy system?* Journal of Power Sources, 2006. **161**(1): p. 474-483.

[10] Y. Iwase, A. Kudo and R. Amal, "Reducing graphene oxide on a visible-light bivo4 photocatalyst for an enhanced photoelectrochemical water splitting," Journal of Physical Chemistry Letters, vol. 1, no.17, **2010**, pp. 2607–12.

[11] J. Davies, "Hazardous Gas Model Evaluation with Field Observations." Atmospheric Environment, vol. 29, no. 3, 1995, pp. 456–457.

[12] Rahimnejad, M., et al., *Microbial fuel cell as new technology for bioelectricity generation: A review.* Alexandria Engineering Journal, 2015. **54**(3): p. 745-756.

[13] Lu, Y., et al., *Solid oxide fuel cell technology for sustainable development in China: An over-view.* International Journal of Hydrogen Energy, 2018. **43**(28): p. 12870-12891.

[14] W. Ning, D. Hui, Z. Xiangyang and M.Yang "Homogeneous Coating of Au and SnO2 Nanocrystals on Carbon Nanotubes via Layer-by-Layer Assembly: a New Ternary Hybrid for a Room-Temperature CO Gas Sensor." Chemical Communications, no. 46, 2008, p. 6182.

[15] Li, X. and A. Faghri, *Review and advances of direct methanol fuel cells (DMFCs) part I: Design, fabrication, and testing with high concentration methanol solutions.* Journal of Power Sources, 2013. **226**: p. 223-240.

[16] Reimer, L., *Scanning electron microscopy: physics of image formation and microanalysis*. Vol. 45. 2013: Springer.

[17] Holade, Y., et al., *New preparation of PdNi/C and PdAg/C nanocatalysts for glycerol electrooxidation in alkaline medium.* Electrocatalysis, 2013. **4**(3): p. 167-178.

[18] Smith, B.C., *Fundamentals of Fourier transform infrared spectroscopy*. 2011: CRC press.

[19] Byrappa, K. and M. Yoshimura, *Handbook of hydrothermal technology*. 2012: William Andrew.

[20] Laudise, R., *the growth of single crystals. Solid state physical electronics series.* Prentice-Hall, Inc, 1970.

[21] Hummers Jr, W.S. and R.E. Offeman, *Preparation of graphitic oxide.* Journal of the american chemical society, 1958. **80**(6): p. 1339-1339.

[22] Ciszewski, M. and A. Mianowski, *Survey of graphite oxidation methods using oxidizing mixtures in inorganic acids.* Chemik, 2013. **67**(4): p. 267-274.

[23] Shahriary, L. and A.A. Athawale, *Graphene oxide synthesized by using modified hummers approach.* Int J Renew Energy Environ Eng, 2014. **2**(01): p. 58-63.

[24] Scott, K., W. Taama, and J. Cruickshank, *Performance and modelling of a direct methanol solid polymer electrolyte fuel cell.* Journal of Power Sources, 1997. **65**(1-2): p. 159-171.

[25] Mekhilef, S., R. Saidur, and A. Safari, *Comparative study of different fuel cell technologies.* Renewable and Sustainable Energy Reviews, 2012. **16**(1): p. 981-989.

[26] Liu, J.H., et al., *Highly-optimized membrane electrode assembly for direct methanol fuel cell prepared by sedimentation method.* Journal of power sources, 2004. **137**(2): p. 222-227.

[27] Jahan, M., Z. Liu, and K.P. Loh, *A Graphene oxide and copper-centered metal organic framework composite as a tri-functional catalyst for HER, OER, and ORR.* Advanced Functional Materials, 2013. **23**(43): p. 5363-5372.

[28] Askari, M.B., et al., *One-step hydrothermal synthesis of MoNiCoS nanocomposite hybridized with graphene oxide as a high-performance nanocatalyst toward methanol oxidation.* Chemical Physics Letters, 2018. **706**: p. 164-169.

[29] Hao Yu, E., K. Scott, and R.W. Reeve, *A study of the anodic oxidation of methanol on Pt in alkaline solutions.* Journal of Electroanalytical Chemistry, 2003. **547**(1): p. 17-24.

[30] King, W.D., et al., *Pt−Ru and Pt−Ru−P/Carbon Nanocomposites: Synthesis, Characterization, and Unexpected Performance as Direct Methanol Fuel Cell (DMFC) Anode Catalysts.* The Journal of Physical Chemistry B, 2003. **107**(23): p. 5467-5474.

[31] Oliveira Neto, A., et al., *Electro-oxidation of methanol and ethanol on Pt–Ru/C and Pt–Ru–Mo/C electrocatalysts prepared by Bönnemann's method.* Journal of the European Ceramic Society, 2003. **23**(15): p. 2987-2992.

[32] Tang, H., et al., *Controlled synthesis of platinum catalysts on Au nanoparticles and their electrocatalytic property for methanol oxidation.* Applied Catalysis A: General, 2004. **275**(1): p. 43-48.

[33] Amin, R., et al., *Pt–NiO/C anode electrocatalysts for direct methanol fuel cells.* Electrochimica Acta, 2012. **59**: p. 499-508.

[34] Maiyalagan, T. and F.N. Khan, *Electrochemical oxidation of methanol on Pt/V2O5–C composite catalysts.* Catalysis Communications, 2009. **10**(5): p. 433-436.

[35] Drew, K., et al., *Boosting fuel cell performance with a semiconductor photocatalyst: TiO2/Pt− Ru hybrid catalyst for methanol oxidation.* The Journal of Physical Chemistry B, 2005. **109**(24): p. 11851-11857.

[36] Villullas, H.M., F.I. Mattos-Costa, and L.O. Bulhões, *Electrochemical oxidation of methanol on Pt nanoparticles dispersed on RuO2.* The Journal of Physical Chemistry B, 2004. **108**(34): p. 12898-12903.

[37] Jayaraman, S., et al., *Synthesis and characterization of Pt− WO3 as methanol oxidation catalysts for fuel cells.* The Journal of Physical Chemistry B, 2005. **109**(48): p. 22958-22966.

[38] Li, W., et al., *Preparation and characterization of multiwalled carbon nanotube-supported platinum for cathode catalysts of direct methanol fuel cells.* The Journal of Physical Chemistry B, 2003. **107**(26): p. 6292-6299.

[39] Chen, J., et al., *Platinum catalysts prepared with functional carbon nanotube defects and its improved catalytic performance for methanol oxidation.* The Journal of Physical Chemistry B, 2006. **110**(24): p. 11775-11779.

[40] Girishkumar, G., K. Vinodgopal, and P.V. Kamat, *Carbon nanostructures in portable fuel cells: single-walled carbon nanotube electrodes for methanol oxidation and oxygen reduction.* The Journal of Physical Chemistry B, 2004. **108**(52): p. 19960-19966.

[41] Jha, N., et al., *Pt–Ru/multi-walled carbon nanotubes as electrocatalysts for direct methanol fuel cell.* International Journal of Hydrogen Energy, 2008. **33**(1): p. 427-433.

[42] Lin, Y., et al., *Platinum/carbon nanotube nanocomposite synthesized in supercritical fluid as electrocatalysts for low-temperature fuel cells.* The Journal of Physical Chemistry B, 2005. **109**(30): p. 14410-14415.

[43] Zheng, S.-F., et al., *In situ one-step method for preparing carbon nanotubes and Pt composite catalysts and their performance for methanol oxidation.* The Journal of Physical Chemistry C, 2007. **111**(30): p. 11174-11179.

[44] He, Z., et al., *Electrodeposition of Pt–Ru nanoparticles on carbon nanotubes and their electrocatalytic properties for methanol electrooxidation.* Diamond and Related Materials, 2004. **13**(10): p. 1764-1770.

[45] Deivaraj, T., W. Chen, and J.Y. Lee, *Preparation of PtNi nanoparticles for the electrocatalytic oxidation of methanol.* Journal of Materials Chemistry, 2003. **13**(10): p. 2555-2560.

[46] Zeng, J., et al., *Preparation of carbon-supported core− shell Au− Pt nanoparticles for methanol oxidation reaction: the promotional effect of the Au core.* The Journal of Physical Chemistry B, 2006. **110**(48): p. 24606-24611.

[47] Yang, L., et al., *Au@ Pt nanoparticles prepared by one-phase protocol and their electrocatalytic properties for methanol oxidation.* Colloids and Surfaces A: Physicochemical and Engineering Aspects, 2007. **295**(1-3): p. 21-26.

[48] Chen, D., et al., *Star-like PtCu nanoparticles supported on graphene with superior activity for methanol electro-oxidation.* Electrochimica Acta, 2015. **177**: p. 86-92.

[49] Qiu, J.-D., et al., *Controllable deposition of platinum nanoparticles on graphene as an electrocatalyst for direct methanol fuel cells.* The Journal of Physical Chemistry C, 2011. **115**(31): p. 15639-15645.

[50] Huang, H., et al., *Graphene nanoplate-Pt composite as a high performance electrocatalyst for direct methanol fuel cells.* Journal of Power Sources, 2012. **204**: p. 46-52.

[51] Vu, T.H.T., et al., *Solvothermal synthesis of Pt-SiO2/graphene nanocomposites as efficient electrocatalyst for methanol oxidation.* Electrochimica Acta, 2015. **161**: p. 335-342.

[52] Zhao, Y., et al., *Enhanced electrocatalytic oxidation of methanol on Pd/polypyrrole–graphene in alkaline medium.* Electrochimica Acta, 2011. **56**(5): p. 1967-1972.

[53] Dong, L., et al., *Graphene-supported platinum and platinum–ruthenium nanoparticles with high electrocatalytic activity for methanol and ethanol oxidation.* Carbon, 2010. **48**(3): p. 781-787.

[54] Ji, Z., et al., *Reduced graphene oxide supported FePt alloy nanoparticles with high electrocatalytic performance for methanol oxidation.* New Journal of Chemistry, 2012. **36**(9): p. 1774-1780.

[55] Furukawa, H., et al., *The chemistry and applications of metal-organic frameworks.* Science, 2013. **341**(6149): p. 1230444.

[56] Yaghi, O. and H. Li, *Hydrothermal synthesis of a metal-organic framework containing large rectangular channels.* Journal of the American Chemical Society, 1995. **117**(41): p. 10401-10402.

[57] Kondo, M., et al., *Three-Dimensional Framework with Channeling Cavities for Small Molecules:{[M2 (4, 4'-bpy) 3 (NO3) 4]· xH2O} n (M□ Co, Ni, Zn).* Angewandte Chemie International Edition in English, 1997. **36**(16): p. 1725-1727.

[58] Li, H., et al., *Establishing microporosity in open metal− organic frameworks: gas sorption isotherms for Zn (BDC)(BDC= 1, 4-benzenedicarboxylate).* Journal of the American Chemical Society, 1998. **120**(33): p. 8571-8572.

[59] Rosi, N.L., et al., *Hydrogen storage in microporous metal-organic frameworks.* Science, 2003. **300**(5622): p. 1127-1129.

[60] Furukawa, H., et al., *Ultrahigh porosity in metal-organic frameworks.* Science, 2010. **329**(5990): p. 424-428.

[61] Yoon, M., et al., *Proton conduction in metal–organic frameworks and related modularly built porous solids.* Angewandte Chemie International Edition, 2013. **52**(10): p. 2688-2700.

[62] Shigematsu, A., T. Yamada, and H. Kitagawa, *Wide control of proton conductivity in porous coordination polymers.* Journal of the American Chemical Society, 2011. **133**(7): p. 2034-2036.

[63] Hurd, J.A., et al., *Anhydrous proton conduction at 150 C in a crystalline metal–organic framework.* Nature chemistry, 2009. **1**(9): p. 705.

[64] Li, Q., et al., *Approaches and recent development of polymer electrolyte membranes for fuel cells operating above 100 C.* Chemistry of materials, 2003. **15**(26): p. 4896-4915.

[65] Stock, N. and S. Biswas, *Synthesis of metal-organic frameworks (MOFs): routes to various MOF topologies, morphologies, and composites.* Chemical reviews, 2011. **112**(2): p. 933-969.

[66] Huang, L., et al., *Synthesis, morphology control, and properties of porous metal–organic coordination polymers.* Microporous and mesoporous materials, 2003. **58**(2): p. 105-114.

[67] Cravillon, J., et al., *Rapid room-temperature synthesis and characterization of nanocrystals of a prototypical zeolitic imidazolate framework.* Chemistry of Materials, 2009. **21**(8): p. 1410-1412.

[68] Kreno, L.E., et al., *Metal–organic framework materials as chemical sensors.* Chemical reviews, 2011. **112**(2): p. 1105-1125.

[69] Fujita, M., et al., *Preparation, clathration ability, and catalysis of a two-dimensional square network material composed of cadmium (II) and 4, 4'-bipyridine.* Journal of the American Chemical Society, 1994. **116**(3): p. 1151-1152.

[70] Wu, C.-D., et al., *A homochiral porous metal− organic framework for highly enantioselective heterogeneous asymmetric catalysis.* Journal of the American Chemical Society, 2005. **127**(25): p. 8940-8941.

[71] Wang, C., K.E. DeKrafft, and W. Lin, *Pt nanoparticles@ photoactive metal–organic frameworks: efficient hydrogen evolution via synergistic photoexcitation and electron injection.* Journal of the American Chemical Society, 2012. **134**(17): p. 7211-7214.

[72] Yuan, B., et al., *A highly active heterogeneous palladium catalyst for the Suzuki–Miyaura and Ullmann coupling reactions of aryl chlorides in aqueous media.* Angewandte Chemie International Edition, 2010. **49**(24): p. 4054-4058.

[73] Lin, S., et al., *Adsorption behavior of metal–organic frameworks for methylene blue from aqueous solution.* Microporous and Mesoporous Materials, 2014. **193**: p. 27-34.

[74] Haneef, M., H. Saleem, and A. Habib, *Use of graphene nanosheets and barium titanate as fillers in PMMA for dielectric applications.* Synthetic Metals, 2017. **223**: p. 101-106.